HAVE LAND USE CHANGES AND ANTHROPOGENIC MODIFICATIONS OF ESTUARIES RESULTED IN CHANGE IN ESTUARINE CONVERGENCE IN SOUTH KOREA?

A Thesis

by

VICTORIA LEE BARTLETT

Submitted to the Office of Graduate and Professional Studies of
Texas A&M University
in partial fulfillment of the requirements for the degree of

MASTER OF MARINE RESOURCES MANAGEMENT

Chair of Committee,	Timothy Dellapenna
Co-Chair of Committee,	David Retchless
Committee Member,	Wesley Highfield
Head of Department,	Kyeong Park

August 2019

Major Subject: Marine Resources Management

ABSTRACT

Estuaries have played a major role in the movement of people, goods and services, and knowledge, as societies have developed over time. They are crucial ecosystems for storm buffering and biological resources. The health and viability of these delicate systems has become increasingly compromised as coastal development and the construction of anthropogenic structures has rapidly increased over the last three decades. The results of anthropogenic modifications of estuaries can be studied through the change of the convergence length over time. However, this process is mathematically involved and would require a lengthy amount of time. Therefore, the aim of this study is to automate the process of calculating the convergence length, in order to analyze the global change of estuaries quickly using ArcGIS and R Coding Software. The primary focus area will be South Korea, as this area has experienced intense dam construction along its major rivers in a short amount of time. Preliminary results suggest that estuaries have changed as a result of the construction and addition of anthropogenic structures.

DEDICATION

To my family and friends who have continued to believe in me and push me to fight for my dreams.

ACKNOWLEDGEMENTS

I would like to thank my committee chair, Dr. Tim Dellapenna for always believing in me and for always telling me what I needed to hear, even if it wasn't what I wanted to hear. Thank you for your support through this process.

Many thanks to my co-chair, Dr. Retchless, for guiding me through this research process. Your advice has been invaluable. In addition, Dr. Highfield, thank you for being a great mentor.

Thanks to my family and friends who have kept me going and helped me see through this process to the end. I don't know where I would be without your love and encouragement.

CONTRIBUTORS AND FUNDING SOURCES

Contributors

This work was supervised by a thesis committee consisting of Dr. Dellapenna [Advisor] and Dr. Retchless [Co-Advisor] of the Department of Marine Sciences and Dr. Highfield of the Department of Land and Urban Planning.

The R Code used for data analysis was provided by Gareth Davies of Wollongong University and was modified for this research project by Chengxue Li of the Department of Marine Biology. The data used for analysis was supplied by Nicholas Wellbrock and Jace Hodder of the Department of Marine Sciences.

All other work conducted for the thesis was completed by the student independently.

Funding Sources

Graduate study was supported by a Teaching Assistantship from Texas A&M University at Galveston and a Research Assistantship from Texas A&M University and Galveston.

TABLE OF CONTENTS

Page

LIST OF FIGURES

Page

LIST OF TABLES

Page

1. INTRODUCTION

1.1. Estuarine Importance

Estuaries have been crucial to the diaspora of people, knowledge, and goods and services. Estuaries provide the natural connection between land and sea, providing a plethora of services to society, including storm protection, nursery grounds for both shell and finfish fisheries, and easy access to the ocean (Wolanski et al., 2019). Also due to this exceptional link, estuaries contain some of the most biologically, socially, and economically important ecosystems in the world and as such, many civilizations that have settled close by have flourished for centuries (Barbier et al., 2011; Martinez et al., 2007). Approximately 50% of global population live within 100 km of the coastline, representing about 80-100% of the populations of over half of the world's coastal countries (Little et al., 2017; Martinez et al., 2007). Moreover, the world's population continues to grow exponentially, creating a greater need for these services, complicated by anthropogenic change causing the destruction of necessary natural elements of these systems, limiting their ability to provide (O'Meara, 2016). The global decline of estuaries through anthropogenic, human-linked causes is intensifying, and over 60% of coastal vegetated ecosystems have been lost due to activities such as changes to the hydrologic cycle and water flow regime within estuaries (Little et al., 2017). For this reason, it is vital that humans maintain the integrity of natural estuarine systems and their associated ecosystem services, which are being threatened by the construction of dams, dikes, and seawalls (e.g. Williams et al, 2013; Williams et al., 2014).

The problem of natural function loss of estuaries through human alteration is compounded by increases in sedimentation rates and even causes the formation of localized

geomorphic features over time (e.g. barrier islands, flood tidal deltas, bayhead deltas). Research has shown that the estuarine end of a distributary system may shoal much more rapidly relative to its upstream riverbed (Zhu et al, 2017). The new influx of sediment, in addition to shoaling can also cause a narrowing of the estuary as well as a change to the bottom type, i.e., converting a mud dominated bottom to a sand dominated bottom or vice versa (e.g. Williams et al., 2013). The changing of the bottom sediment type can dramatically alter the ecosystem and ecosystem services, as benthic and epibenthic organisms are dependent on specific substrates, for example, *Mercenaria mercenaria* depends on a substrate with a relatively high sand content and *Macomoa baltica* and *Cyrtopleura costata* require mud bottoms. In addition, elevated sedimentation rates can impact both the abundance and diversity of benthic communities (e.g. Nassar, 2011; Chou et al., 2004). Field and laboratory experiments by Norkko et al., (2002), Cummings et al., (2003), Hewitt et al. (2003) and Thrush et al. (2003a&b), summarized by Thrush et al. (2004) reveal that a critical threshold of episodic deposition of 2 cm deposits in an estuary will quickly create anaerobic conditions within the seabed, resulting in the death of the resident faunal community. The benthic and pelagic coupling within an estuary is central to the nutrient cycling and overall productivity of the system and an interruption of this coupling resulting from elevated sedimentation rates can have dramatic impacts on the entire ecosystem (Eyre and Ferguson, 2006).

From a geomorphic perspective, high sedimentation rates can result in shoaling of estuaries, as well as narrowing or convergence of estuaries. The loss of estuarine area reduces the volume of the tidal prism, and results in a feedback loop where the reduction in tidal flushing permits additional sediment retention within the estuary (e.g. Williams et al., 2013 and 2014), all of which also affect the ecosystem servicing of the estuary. One way to study this affect is by

observing the convergence length of an estuary over time. Convergence is the narrowing of an estuary, i.e. the convergence of the estuarine banks. Convergence length is the distance over which convergence occurs, usually in an exponential manner by a factor of e ≈ 2.718282 (Davies and Woodroffe, 2010). This convergence length has been traditionally calculated using the following equation (Langbein, 1963; Lanzoni and Seminara, 1998; Savenije, 2005; Davies and Woodroffe, 2010):

$$B(s) \approx We^{-\frac{s}{L_b}}. \quad (1)$$

In equation 1 above, *s* signifies a centerline, arc length coordinate falling upstream of the mouth, *B(s)* is the width of the estuary at coordinate *s*, *W* is an approximation of the width at the mouth and L_b is an approximation of the estuarine convergence length. The convergence length is controlled by a number of factors, including sedimentation rate (Dronkers, 2017). However, as described by Dronkers (2017) in "Convergence of estuarine channels," calculating estuary convergence is a lengthy process, plagued with uncertainty, assumptions, and approximations, in which he cautions the reader to consider before application to other estuaries. For example, in Dronkers' study, the convergence lengths of 21 estuaries around the world were analyzed. However, the hydrodynamic model used to evaluate the equilibrium state of the estuaries was simplified so that some nonlinear factors were made negligible and some were linearized. This changed the overall validity of the model, so only estuaries with a constant depth and an exponentially decreasing width could be analyzed (Dronkers, 2017). However, this very rarely occurs naturally. Many other models experience the same problem; making generalizations in order to obtain a result. Some of these include: Savenije (2005) and Chappell and Woodroffe (1994), seen below in equations 2 and 3, respectively. As with the Dronkers model, both of these models assume constant depth, width, discharge, etc. While the results may be similar to

observed convergence lengths within estuaries, the amount of uncertainty warrants some apprehension.

(2) $$L_b = \frac{\sqrt{gd}}{\frac{8g\|u\|}{3\pi C^2 \underline{d}}}$$

C=Chezy Friction Coefficient

d=Depth

$\underline{d}$=Time-averaged Depth

g=Gravitational Acceleration

$\|u\|$=Tidal Velocity Amplitude

(3) $$L_b = \frac{T\underline{du}}{4a}$$

T=Tidal Period

$\underline{du}$= Width and Time-averaged discharge

a=Tidal Amplitude

For this reason, a metric is needed to analyze convergence length of individual estuaries in a manner in which they can be compared across the board, all mathematical assumptions aside. This tool is needed to rapidly assess a large amount of data, using the geographic location of the estuaries, in complement to the geomorphology or hydrodynamic attributes of the estuaries. This will allow the changes in convergence length to be easily identified, globally, which will aid in pinpointing the causes of estuarine change and allow researchers to create positive change in the declining health of global estuarine systems.

1.2. Project Purpose and Hypothesis

To assess the variations of estuarine convergence and changes in convergence over time, on a regional or global scale, a tool is needed that can quickly process large sets of geospatial data and calculate convergence length of estuaries. Convergence length is the metric that will be used to compare the degree of convergence between individual estuaries. Therefore, the purpose of this research is to develop an algorithmic tool that can be used on estuaries in order to quantify estuarine convergence length between individual estuaries geospatially, as opposed to geomorphologically. The geospatial datasets that will be used as part of this analysis include the Global Surface Water Dataset (GSWD) and the HydroSHEDS Model, both described below. Over half of the estuaries on the Korean Peninsula have undergone significant anthropogenic alterations, as described below. The protocol for quantifying estuarine convergence will be used to test the hypothesis: ***Within the Korea Peninsula, anthropogenic alterations in estuaries has resulted in a statistically significant change in estuarine convergence.*** As explained above, an ideal estuary would lie perfectly on an exponential width per unit distance curve. The measured widths are plotted against this ideal estuary curve and measured for the difference in each width at each distance variable. This difference between the measured widths and the ideal widths is the residual measurement. This is done for each estuary at each time point. For example, the 1985 measured widths for one estuary are plotted with the 1985 ideal estuary curve for that same estuary. An example plot can be seen in figure 1 below. Appendix I contains plots for each analyzed estuary. In further analysis, the widths of the estuary from 1985 are tested against the widths of the same estuary in 2015. A t-test was performed to determine if the means of each collection of widths are statistically different. The null hypothesis for this test is that the means are equal. In terms of net convergence length, if the t-test for an estuary is returned with a

significant *p* value, then the change in the width values is deemed significantly different. It is important to note here that an unpaired t-test was used (Welch two sample t-test), as the sample sizes were unequal for each estuary. In addition to this, a KS test was also performed to assess the equality of the distribution of the width measurements for each year. The null hypothesis for this test is that the distributions between the years are equal. If this test is returned with a significant *p* value, rejecting the null hypothesis, it also indicates that the change in widths is significant.

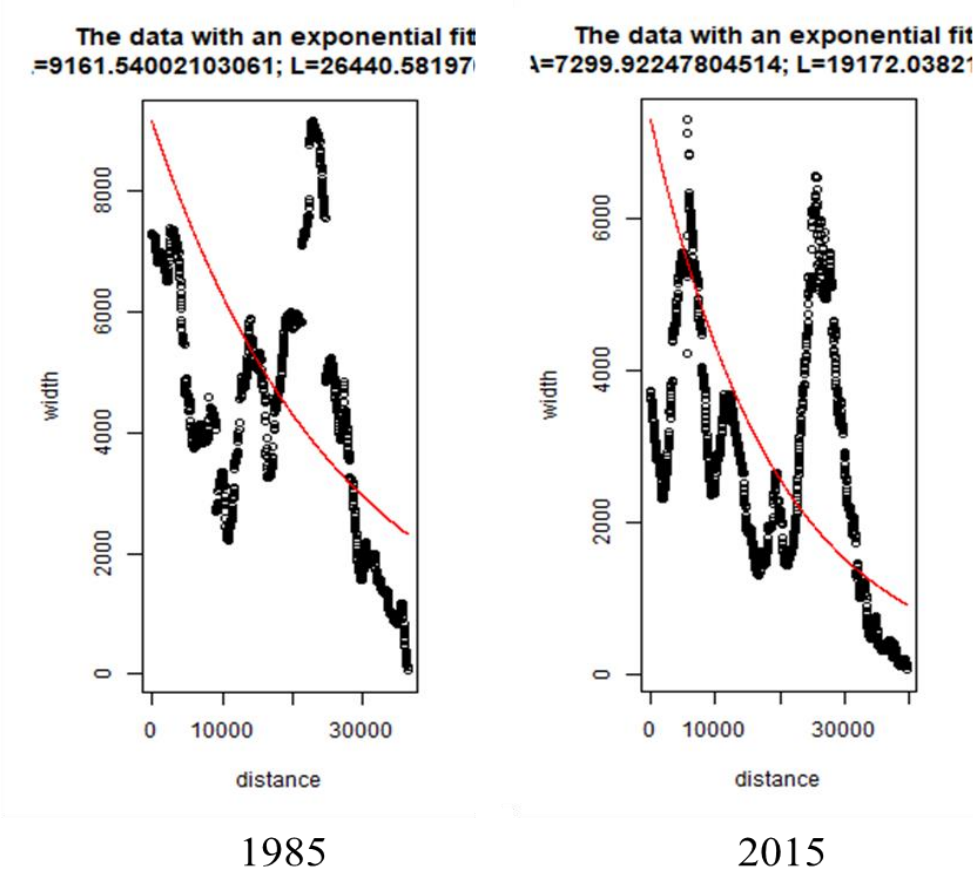

Figure 1 Residual plots of South Yeongsan (E14) Estuary Set from 1985 and 2015. A is the area, L is the convergence length.

2. BACKGROUND

2.1. Study Area

The scope of this project is limited to South Korea as a base model for proof of concept of the calculation of estuarine convergence. The geologic history of the Korean peninsula is quite interesting and unique, lending to its usefulness as the base model for this research. The generally rocky coastline is rather complex, due to the peninsula being submerged during Holocene transgression, following the Last Glacial Maximum (LGM) (Wells et al., 1990). This transgression led to the rocky, crenulated coast mosaicked with bays and estuaries found today (Wells et al., 1990).

Within South Korean, there are three major rivers that each form from the convergence of a series smaller rivers, creating intricate riverine systems (Park and Lee, 2002). The Han River is the largest river within South Korea, at roughly 564 km long and flows towards the Yellow Sea in the west (Chang, 2008). The second largest river in South Korea is the Nakdong River, at 525 km long (Park and Lee, 2002), and the third largest is the Geum at only 131 km (Jeong et al., 2010). Much of the precipitation and associated fluvial input comes during the summer monsoon and the occasional typhoon (Chang, 2008).

Another interesting and unique characteristic of the Korean Peninsula is the variation in tidal ranges from coast to coast. The eastern coast of the peninsula is microtidal, with semi-diurnal tides generally less than 2 meters. The west coast is macrotidal with a semi-diurnal tidal range of 4-6 meters. The southern coastline is mesotidal, with semi-diurnal tides averaging between 2-4 meters (Ryu et al., 2004; Davies, 1964).

In 2011, Lee et al. identified 463 estuaries in South Korea through various methods based on environmental characteristics and land use information. Of these estuaries, they state that 235 of them are considered open (Lee et al., 2011), leaving 228 identified as closed. The closed estuaries are then broken into two categories: blocked (144) and lake type (84) (Lee et al., 2011). A majority of the blocked estuaries are identified this way, on account of the installation of anthropogenic development, such as dams (Lee et al., 2011).

2.2. Estuary Types

There are many diverging definitions to this question, some answering it as "a tongue of the sea reaching inland," (Perillo, 1995) or as simply just the connection between a river and the sea (Pritchard, 1952). Perillo (1995) suggests that not only is estuarine classification a function of the physiographic features, such as geomorphology, hydrology, biological, and chemical characteristics, but is in part, informed by the context in which the research is being conducted. In the context of this research, the primary focus will be on geomorphology and sedimentation, which encompasses several types of estuaries, which are the: 1) drowned river valley; 2) lagoon-type, bar-built; 3) fjord; 4) tectonic action-produced; and 5) rias (Hume et al., 1988; Evans and Prego, 2003).

Drowned river valleys were formed in Pleistocene-Holocene-age river valleys that were flooded by seawater during the Flandrian transgression period (Perillo, 1995). The average depth of these valleys generally ranges from 10-30 m. These estuaries are characterized by the typical 'funnel' shape, which increases rapidly as the mouth approaches. For these estuaries to be maintained throughout their history, the long-term sedimentation rates within these estuaries are equivalent to the local sea level, with the accommodation space created by sea level rise being

filled with sediment, resulting in a balance between the funnel shape and sedimentation/erosion rates leads to a delicate equilibrium (Perillo, 1995).

Bar-built estuaries, also known as coastal lagoons, are heavily influenced by littoral processes. The interaction between these processes and wind allow barriers to be built up along the edges of these estuaries, usually enclosing them. Typically, these estuaries are found in river valleys with extremely low relief, very little river discharge, and small tidal changes (Perillo, 1995). The surrounding environment includes features such as tidal flats, marshes, and mangroves (Perillo, 1995).

Fjords were formed by ice sheets and glaciers during the Pleistocene era and are mainly located in higher latitudes. The formation of these estuaries included a period of time in which a glacier invaded the mouth of a river bed and moved inland over time, carving out deep sections of river bed. Eventually, as the glaciers moved, the river bed was filled with encroaching seawater. For this reason, these estuaries are characterized by very deep channels, in a U-shape. Towards the mouth, there is more coarse-grained sediment, while the bed of the estuary is filled with fine-grained, muddy sediment. The environment adjacent to these estuaries includes rocky shorelines with deficient sediment supply (Perillo, 1995).

Within the tectonic activity classification, there are two main types of estuaries: fault-defined and diastrophic. The former category includes estuaries characterized by long and narrow passageways, with widths being less than 2 km. As indicated by the name, fault systems drive the physical features of the estuaries, including the subparallel shores. The hydrological features of these estuarine types are influenced primarily by the local tides (Hume et al., 1988). The latter category tends to be larger and more expansive estuaries, driven primarily by wind and

oceanic currents, formed through natural, dystrophic processes. Typically, the width of these estuaries is close to 5 km (Hume et al., 1988).

Finally, a ria is geomorphologically similar to an incised river valley. Perillo describes Ria's in his 1995 book as, "a former fluvial valley developed in high relief (mountainous of cliffy coast)," (Perillo, 1995). Typically, these river valleys have been filled in over time through relative sea level rise occurring postglacially. The shape of these estuarine types is characteristically seen as either trumpet shaped or the typical funnel shape (Fairbridge, 1968). This type of estuary is the most prevalent along the South Korean coastline.

2.3. Anthropogenic Impacts on Estuaries

Rice farming in South Korea is dated back to around 1500 BC, beginning with simple irrigation techniques, such as gravity-influenced terraces that were constructed at the bottom of hills to receive water from higher elevations. In addition, rice fields were elevated in order to extort the use of the high water table (Crawford and Lee, 2003). One key aspect of the terraced agriculture is that it both controls the flow of water as well as sediment, trapping much of the sediment within the terraces rather than flowing into the fluvial systems. Consequently, the construction of these elevated rice fields can be argued as one of the starting points of the anthropogenically engineered drainage basin, leading to a feedback loop in the natural system that resulted in a divergence from the natural, unaltered system. Over time, as these practices were refined and coastal development increased, the natural drainage patterns and movement of sediment throughout drainage basins (and ultimately estuarine) were altered. Yoon et al. (2007) stated that as a result of coastal development, river obstruction lead to a reduced rate of water flow, which in turn, lead to increased sedimentation on the lower reaches of the waterway. A study conducted by Gao et al. in 2015 found that the anthropogenic changes along within the

Changjiang catchment in China caused the sediment load of the upstream portion of the river to be reduced, which significantly changed the erosion/depositional scheme of the lower portion of the river. Overall, the changes have altered the sedimentation patterns of the river, completely reversing the role of the lower portion from sediment sink to sediment source for the open ocean (Gao et al., 2015).

In further evidence, the major rivers of South Korea have experienced immense change over the course of the past several decades. In the 1930's, construction on two dams along the estuarine portion of the microtidal Nakdong River were completed. One of these dams also included a seawall along the downstream portion. However, after construction, the dams were seldom, if ever opened, cutting off both the freshwater as well as sediment delivery to the estuary below (Williams et al, 2013). The Nakdong Estuarine Dam started construction in 1983 and finished in 1987. This dam has been operational since its inception. Additionally, part of the construction of this dam included a 2 km long seawall, starting at the dam and moving seaward (Williams et al, 2013). These alterations along the Nakdong River have resulted in a 10-fold increase in sedimentation rate below the dam (Williams et al, 2013). Within the macrotidal Yeongsan estuary, a large estuarine dam was installed in 1981 and Williams et al (2014), discovered that upon construction of the Yeongsan estuarine dam, the sedimentation rate again increased by a factor of 10 within the estuary below the dam. In each system, this increase in sedimentation is thought to have been spurred by the loss of the tidal prism after the dam was installed (Williams et al., 2014 and 2013). These dramatically elevated sedimentation rates, in addition to shoaling, would likely have also caused the narrowing, or convergence of the estuary.

The introduction of estuarine dams into South Korea took place during the Japanese Colonial Period from 1910 to 1945. The Japanese began mimicking hydroelectric and

irrigational dam construction seen in the US at this time. A majority of the hydroelectric dams were concentrated in the northern portion of South Korea, where industrial development was blossoming, while irrigation dams were built in the southern part of the country to supplement land cultivation practices. This was driven by the need to supply food and industrial materials to the Japanese Army during the Second World War. After South Korea gained its independence from Japan in 1945, North Korea cut off the electrical power supply, leaving the South Koreans with 50 percent less power. This, in turn, caused the South Koreans to rely heavily on hydroelectric dams to meet their growing power demand, revitalizing the ones already in place, and ramping up construction on new dams (Choi et al., 2017). Because of the heavy reliance on dam construction within South Korea and the realized impacts of this construction on estuarine environments, it is expected that estuaries with similar geomorphologies and characteristics as the ones described above will have comparable results when anthropogenic dams are constructed.

2.4. Data

The data used for this research project was initially cultivated from the Global Surface Water Dataset (GSWD), produced by Pekel et al. (2016) through the Google Earth Engine interface. This dataset provides measurements of global surface water from 1984-2015. Hodder (2018) developed an algorithm to trim the GSWD to include only coastal embayments. He also developed an algorithm to identify which of those embayments may be considered estuaries based on the proximity of the GSWD data to data contained within the HydroSHEDS (Hydrological data and maps based on Shuttle Elevation Derivatives at multiple Scales) model from the World Wildlife Fund (WWF, 2017), which contains river and stream data and applied these algorithms to the coast of South Korea (Hodder, 2018). The process Hodder (2018)

developed allows for the identification of estuaries based on their proximity to rivers and streams via their modification by using an algorithm built within Google Earth Engine (GEE) and ArcGIS. This algorithm accesses and isolates the pre-processed surface waters within GEE using a block of code developed to pinpoint permanent surface waters of a specific country based upon the countries exclusive economic zone and the maximum extent of water within a particular year between 1985 and 2015. Data derived from the GEE code block is then imported to ArcGIS to be managed by a series of geoprocessing tools. The first of these was a series of small buffers comprised of 200 meters and -200 meters to smooth artifacts left due to the high resolution of the original surface water data. At this point, "holes" within the data were then deleted using the Eliminate Polygon Parts (EPP tool to eliminate landmasses which may obstruct the process). An erase tool was then applied on a combination of the 200-meter buffer result and EPP to further eliminate islands. A large polygon was then manually drawn around South Korea at approximately 1000 kilometers from the coast in order to prevent an error associated with future buffering on a larger scale. This polygon and the previous polygon created with the erase tool then had a Union and Dissolve tool applied to them to join them as one large mass. A buffer series with a 25-kilometer size was then applied to this result, with a negative 25-kilometer buffer applied first, and a positive 25-kilometer buffer being applied second. This result was then erased from the EPP results in order to find embayed areas. These "embayments" then had a Multipart to Singlepart tool applied to them in order to divide them into separate features. A stream dataset (HydroSHEDS) was then imported into the ArcGIS, streams with an "UPCELL" count of 1000 were selected, and the results were then exported to a new shapefile. However, this process excluded a majority of the estuaries within South Korea, and was updated in the process described below to include all streams. This refined stream data set was then used to

select embayment polygons which intersect the stream data or are within 1 kilometer of said polygon. By the operational process of Hodder's (Hodder, 2018) algorithm, an estuary is defined as an embayed, isolated area of permanent surface water determined by the application of a 200 meter and 5 kilometer buffer series which comes in contact with or is within proximity of (≤1 km) a stream with an "UPCELL" count of 1000 kilometers or greater. These areas may include either a singular estuary or may comprise an estuarine system with multiple estuaries.

However, since the Hodder thesis was written in 2018, changes have been made to the pre-process which are reflected in the data obtained for this research. The primary changes to Hodder's algorithm involved refining the actual automation of the ArcGIS process via ArcGIS Model Builder and the use of Natural Earth's Cultural Large scale data, 1:10m to delineate landmasses. The automation is important from three perspectives as it 1) reduces the chance of human error caused by performing each function repeatedly, 2) streamlines the process to enable faster testing which requires little to no interaction during processing time, and 3) is the first step in applying the process on a global scale. From a testing perspective it also allows the swapping out of various tools and settings without having to repeat the entire process. This automated process was split into two separate models. The first of these is known as the "landmass separator", which uses a combination of the landmass data and stream data to determine if a particular landmass contains a stream, keeping those which do, and then separating each singular, separate landmass into its own shapefile. These shapefiles are then fed into the second model which performs the bulk of the estuary identification process. The key item included in this step, which was not located in Hodder's tools, was an iterator. The iterator allowed the entire process to be run repeatedly on each individual landmass, identifying a set of estuaries within each, while not having to restart the process each time the model completed a singular landmass.

Within this same model a variety of new functions were added on top of Hodder's in order to increase accuracy and the diversity of locations, globally, which the algorithm may be applied. The first of these was the automation of drawing the so called "large polygon" around the study area to prevent overlapping errors caused by narrow, negatively buffered areas. This automatically drawn "large polygon" reduced the possibility of human error, allowing for consistency for each landmass. The changes also included a verification process for landmasses, which included eliminating an error where landmasses within close proximity to each other would "latch" onto one another and create false representations of embayments and eventual estuaries. The resulting data was supplied as a shapefile containing a polygon of all identified estuaries within South Korea. Additional data needed for this research that was included with the estuary data, is a 5 km buffer polygon shapefile, which was used to trim the surface water down to estuarine waters and this was coupled with the multipart to singlepart tool to individualize each polygon into individual estuaries. This allows the final product to contain only individual estuary polygons and not one polygon feature containing all the estuaries.

Additionally, an 'R' code block was provided for post-processing of the geographical data to calculate convergence. This code was developed and supplied by Gareth Davies (Davies & Woodroffe, 2010). He supplied the preliminary code for this research in the spring of 2018. The code was then modified by Bartlett with help from Chengxue Li at Texas A&M University-Galveston Campus to process data from the ArcGIS outputs. The slight modifications included a line which selects a 'beginning point' automatically from the input dataset. Additionally, the code also selects plot parameters for the output graph, based on the dataset.

If you are including any previously published articles, or parts of articles, then you'll likely need to submit a copyright permission and add a citation within the text.

3. METHODOLOGY

Using the estuary data files created by the updated Hodder (2018) algorithm, the first step is to process the data in ArcGIS. This was automated using the ArcGIS ModelBuilder Software, which reduces human error by allowing each estuary to be processed exactly the same. The polygon dataset must be converted to points in order to run through the code used for convergence length calculation within the 'R' Software. In order to do this, three models were created. The first of these is the Reproject Model, used to transfer the polygon data from one coordinate system to another. The next model is the Split Model, used to break each estuary into individual shapefiles, and finally, the Data Processing Model, used to convert the polygon data to point data. Each step is described in depth below.

3.1. ArcGIS

3.1.1. Reproject Model

Before the processing of the data begins, the shapefiles need to be projected into the coordinate system 'WGS_1984_UTM_Zone_52S' using the 'Project' tool. This is done because the 'R' Code will only process the data in a projected coordinate system. The UTM coordinate system was selected because of its versatility on a global scale. It can easily be applied to places all around the world. The input data was received in the WGS 1984 Datum, so this datum was used. The linear unit for this coordinate system is meters.

3.1.2. Split Model

The next step is to split the estuary polygon data ('possibleEstuaries') into separate shapefiles for each individual identified estuary in South Korea. This is done by first using the 'Polygon to Line' tool to convert the polygon data into line data for easier processing. The input

for the tool is the ‘possibleEstuaries’ shapefile and the output is a shapefile with line data, outlining the shape of the estuaries for conversion to points later. This file is named ‘SK_PolytoLine_3.’ The next step is to perform the split, by using the ‘Split’ tool, in order to process each estuary by itself, without the influence of the other estuaries surrounding them. The input of this tool is the ‘SK_PolytoLine_3,’ which is being split by the ‘possibleEstuaries’ shapefile. The split field is ‘SplitInput,’ which is a unique identifier of each estuary (Fig. 2). For this process, it is just the FID number, converted from Object ID field type to String field type, which is a requirement of the ‘Split’ tool. The outputs of this tool are shapefiles containing one outline of an estuary per shapefile, which are named after the ‘SplitInput’ for that estuary. They are placed in a target workspace, which is titled ‘ModelOutputs_NewData.’

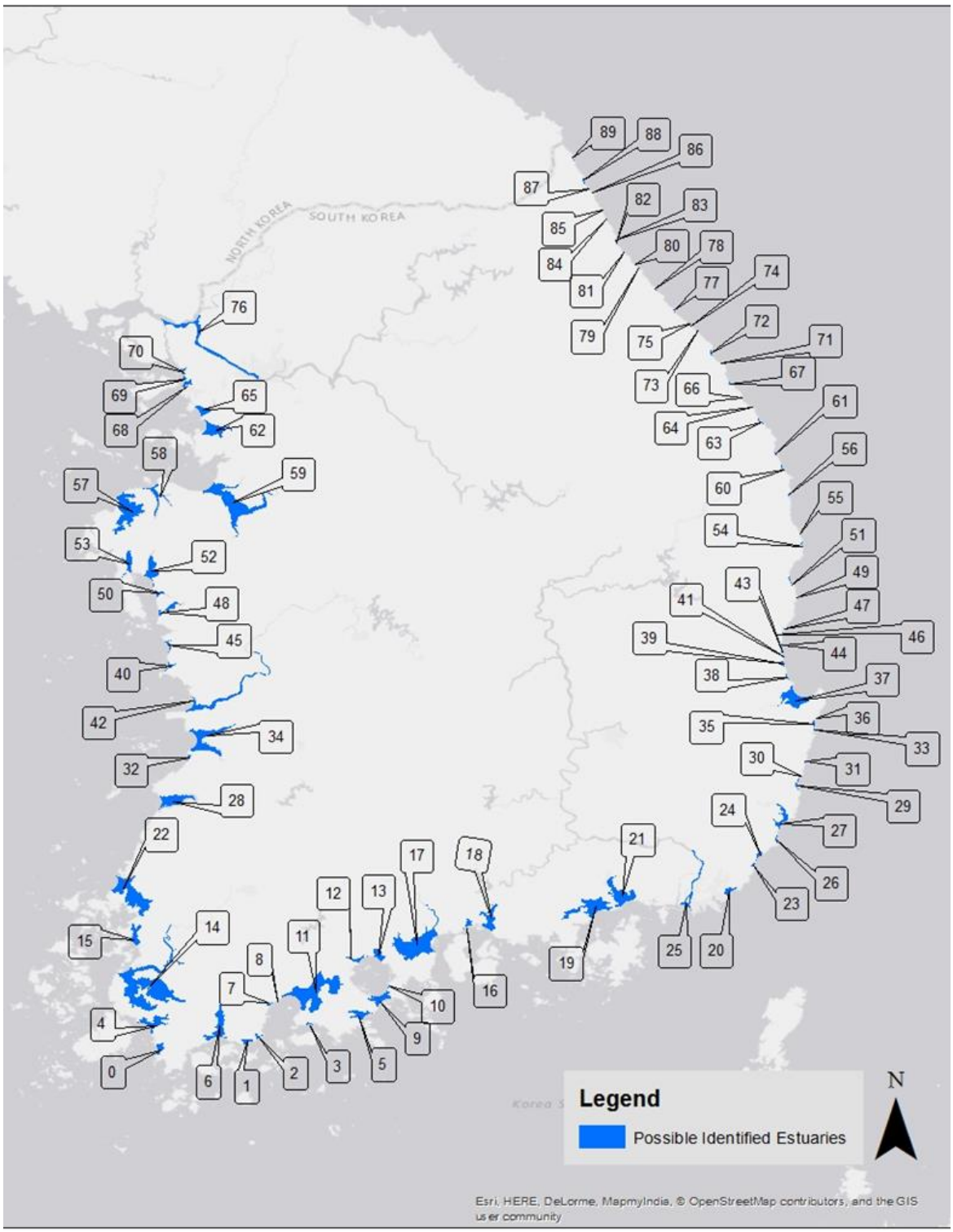

Figure 2 A map depicting the location of the possible identified estuaries on mainland South Korea in 1985. Once split, the estuaries take on the number labelled in this map as their 'SplitInput'.

3.1.3. Data Processing Model

The output workspace of the Split Model is then run through the ‘Workspace or Feature Dataset’ model iterator. The purpose of this is to run all of the shapefiles through the process automatically, without having to go back and process each estuary by hand. The outputs of the iterator include a name output, which names each shapefile based on the ‘SplitInput,’ and the shapefile of the estuary lines. For example, the output of the iterator after running the first estuary shapefile is ‘0.shp’ as the ‘SplitInput’ field for the first estuary in the ‘possibleEstuaries’ shapefile is ‘0.’ The following describes each step of this model in detail:

3.1.3.1. Erase

The previously created shapefile is used as an input for the next step of the process, which is to erase the part of the line that runs across the mouth of the estuary, using the ‘Erase’ tool. This is an important step that must be completed before points are generated due to the fact that the points must be numbered in a very specific way. The ‘5kmBuffer’ shapefile is also input into the ‘Erase’ tool as the erase feature. This polygon shapefile is a buffer off the coast of South Korea, which cuts into the estuaries, in order to remove the line across the mouth, without compromising the width of the mouth. Figure 3 depicts this process. The output for this tool is a shapefile of the outline of an estuary without a line across the mouth, named ‘%Name%_Erased.’ The ‘%Name%’ is the identifier of the ‘SplitInput,’ which signifies the estuary that is being run through the process.

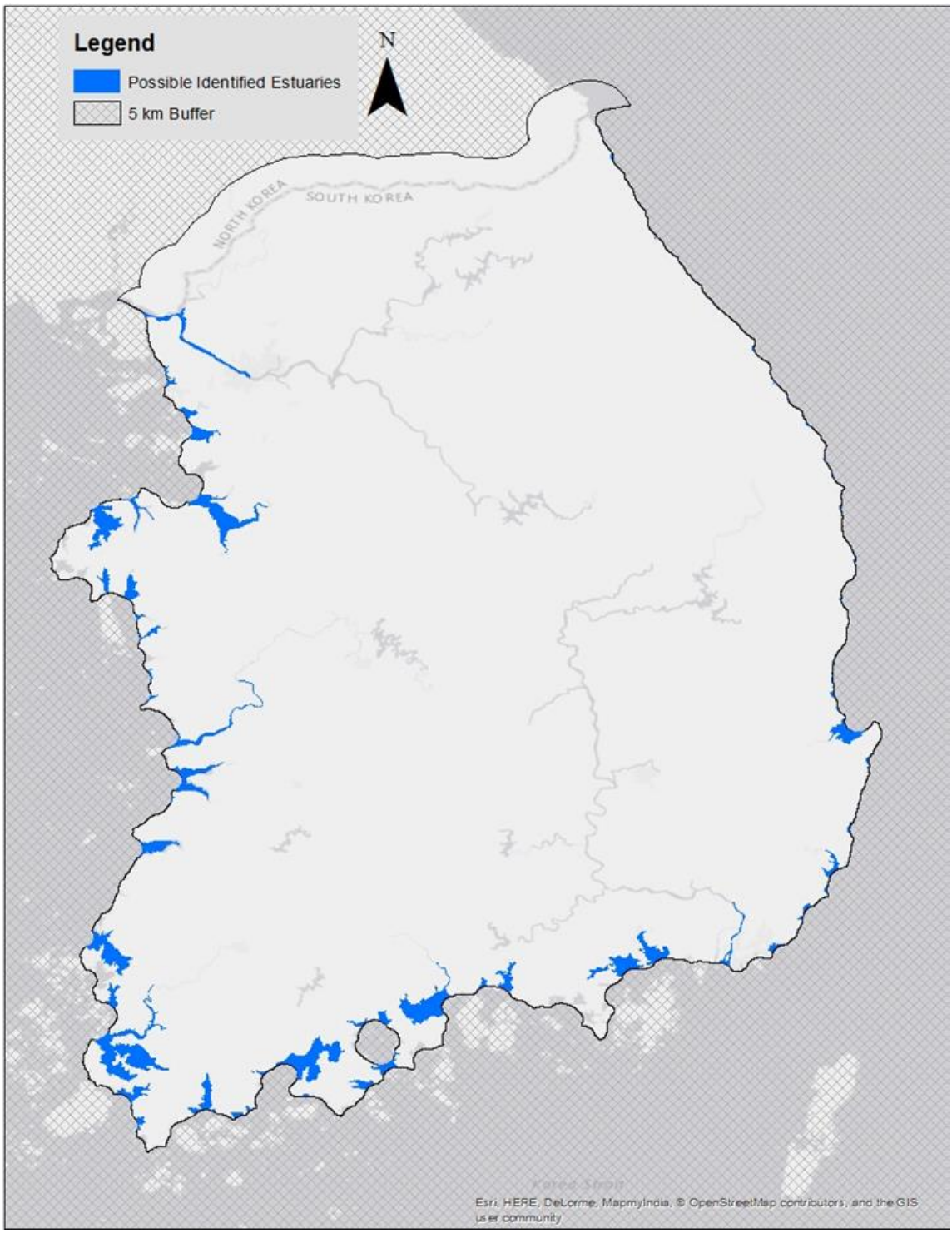

Figure 3 Selection of line across the mouth, using the 5 km buffer.

3.1.3.2. Generate Points Along Lines

The '%Name%_Erased' is the input for the next step in the process, which is the 'Generate Points Along Lines' tool. This creates points along the estuary lines, spaced 25 meters apart, which was the spacing defined within the R Code supplied by Davies. Within the context of the Davies & Woodroffe study, the estuaries were manually digitized within ArcGIS at a scale between 1:6000 and 1:10000, in which points were placed 2 pixel widths apart (12.5 x 12.5 m^2 pixels) along the banks of the estuaries. The points must begin at one end of the estuary and end on the other side (i.e. point on Bank 1 starts at 0, and the very last point on Bank 2 is the last sequential number in the set). This is done because the data processing done in R has a specific format for the input dataset. The points must be processed in sequential order. The output is titled '%Name%_Points'.

3.1.3.3. Add XY Coordinates

The '%Name%_Points' are then input into the 'Add XY Coordinates' tool. This is done for accurate georeferencing within 'R.' The output of this tool is also titled '%Name%_Points.' It is important to note here that the UTM coordinates define the geographical positions of these points in the UTM Zone 52S coordinate system.

3.1.3.4. Copy Features

At this point, the data contains all the information necessary for the R code, however the data needs to be divided by bank. This portion of the process is crucial to the project, as the R Code is written in such a way that each bank of the estuary is input separately. In order to do this, the first step is to break each estuary into two banks, either North/South or East/West, depending on orientation of the estuary. There are very specific steps that need to be followed within ModelBuilder for the process to be automated. This step requires the use of the 'Copy Features'

tool, which creates a new shapefile containing all the information. The importance of this is that now the attribute table can be manipulated in the next step.

3.1.3.5. Add Field

In this step, a field is added to the attribute table of the '%Name%_Points' shapefile. The field, 'PN', is the numbering system used for the points along the estuary. This is very important as the points have to be numbered consecutively along the estuary.

3.1.3.6. Calculate Field

The 'PN' field created previously is calculated using the 'Calculate Field' tool. The expression used within the tool is given below. This was done so that the numbering of the points began with 1, instead of 0.

PN = [FID]+1

3.1.3.7. Near

In this step, the midpoint of the estuary is determined using the 'Near' tool. This tool produces a shapefile with distance information in the attribute table, including the distance of each point from the input data. For this research, it was decided by Bartlett and Retchless that the point with the greatest distance from both endpoints could be considered the midpoint. In order to do this the following process was included in the model:

3.1.3.7.1. Make Feature Layer

This turns the '%Name%_Points' shapefile into a selectable layer.

3.1.3.7.2. Select Layer by Attribute

This tool is used to select only the endpoints of the estuary, using the following expression:

"PN" = 1 OR "PN" = %Row Count%

The %Row Count% is a number generated by the ‘Get Count’ tool, which is used to select the last point on the attribute table for each estuary. This approach was used because each estuary has a different number of points. The output of the ‘Get Count’ tool was set as a parameter of the ‘Select Layer by Attribute’ tool, in order for ModelBuilder to process the ‘Get Count’ tool first.

3.1.3.7.3. Copy Features

This tool is used to copy only the selected endpoints into a new shapefile.

3.1.3.7.4. Make Feature Layer

This tool converts the shapefile into an editable layer for the next step. The newly created layer, ‘%Name%_2Points’, is used as an input to the ‘Near’ tool, as well as the ‘%Name%_Points’ shapefile.

3.1.3.8. Make Feature Layer

The layer output of this tool includes the distance information and will be used to select the point with the greatest distance from the endpoints. It was named, ‘Dist_%Name%’.

3.1.3.9. Summary Statistics

This tool was used to find the point with the greatest distance (i.e max value in the distance field in the attribute table) from the two endpoints. The output of this was a table containing only that value, ‘Stat%Name%’.

3.1.3.10. Join Field

The ‘Stat%Name%’ table was joined back to the ‘Dist_%Name%’ layer based on the distance field. The resulting shapefile, ‘Stat%Name%, included the distance field as well as a max distance field; however, this field was empty aside from the row with the max distance.

3.1.3.11. Make Table View

This tool created a temporary table from the ‘Stat%Name%’ shapefile. This was done because the ‘Stat%Name%’ layer did not contain the original FID field.

3.1.3.12. Add Join

This step joined the temporary table back to the ‘Dist_%Name%’ layer in order to relate the max distance back to the original FID given to the points.

3.1.3.13. Copy Features

This converted the ‘Dist%Name%’ layer into a shapefile for the next step, which requires a shapefile format.

3.1.3.14. Add Field

This tool was used to add a new field to the attribute table, Dist_PN, which will contain the number of the point which is the farthest distance from the endpoints.

3.1.3.15. Calculate Field

This was used to calculate the Dist_PN field that was just created. The expression used to fill the field is listed below:

[Stat%Name%_PN]

This allows the max distance field to be completely filled out with the same value in every row (the max distance from the endpoints).

3.1.3.16. Add Field

This step is used to add another field, PtNumb, to the attribute. This field represents the point number. This field was created to clean up the data, as the other fields with the point number also contained the source table information (ex: ‘Stat%Name% PN’).

3.1.3.17. Calculate Field

The expression used to calculate the field, PtNumb, is listed below:

PtNumb = [Stat%Name% PN]

3.1.3.18. Make Feature Layer

This step converts the previous shapefile into a layer, in order to use the selection tool in the next step.

3.1.3.19. Select Layer By Attribute

At this point in the process, the model is broken into two separate branches, one for each bank. This tool and the tools that follow will be in terms of Bank 1, but the process is the same for both banks. Difference in process will be noted. The 'Select Layer By Attribute' tool is used in this step to select the points that are greater than or equal to the midpoint for Bank 1, and less than the midpoint for Bank 2. This was done to separate the banks into two individual layers.

3.1.3.20. Copy Features

This tool was used to convert the layer into a shapefile, as the next step requires a shapefile format.

3.1.3.21. Add XY Coordinates

This step was included to clean up the data. The previously created X and Y fields contained source table information and needed to be removed.

3.1.3.22. Table to Table

This tool was used to take the attribute table from the shapefile and convert it to a .csv file for processing in R. This format was chosen because of its ease of use and versatility between programs. Within this tool, all data is deleted from the attribute table with the exception of the XY Coordinate data and the point number field. The order of the fields is also changed so

that the X Coordinate is first, the Y Coordinate is second, and the point number is third. This is the order in which R recognizes each piece of information for the points. The output file is named '%Name%_Bank1.csv' or '%Name%_Bank2.csv', depending on which branch the points are being processed under.

3.2. Excel

In excel, the headers are removed from the data and is double-checked for the proper information, in the correct order. Additionally, ArcGIS created an OID (Object ID) in the background, while saving the .csv file; this column is removed. The data is ready for processing within the R Software System. The file name is not changed.

3.3. R Code

The modifications by Bartlett and Li included automating the process of selecting a begin point for the R Code to start processing. This is a point that lies just off the mouth of the estuary and is centered between the two banks. Another modification needed included automatically setting the boundaries of the plot outputs of the code using the parameters of the input data. This included selecting the maximum and minimum values of both the longitude and the latitude and values lying just outside of the minimum and maximum values for the input dataset. Additionally, a loop function was added to the code which allows the code to cycle through the folder containing all the data files. Once these modifications were completed, the R Code was used to process the .csv files for 1985 and 2015. In order to do this, the working directory was set for either the 1985 or 2015 folder, containing the relevant files. The following expression is then entered into R, which supplies arguments needed for the R Code to run: source('Korea_AnalysisCode.R', echo=TRUE, max.deparse.length=Inf). The outputs of the 'R' Code are plots showing the location of the centerline of the estuary, plots showing the width

calculations, and a plot which shows distance versus width, supplying the convergence length and estimated area of the estuary (Fig. 4). The code processes the points by performing a series of operations that calculate several distances between points on the same bank, as well as the relationship of the points along both banks. These calculations are used to first identify the centerline of the estuary, then the distance of the banks to that centerline. According to a supplemental publication to the 2010 Davies and Woodroffe paper, the centerline was defined within the R Code as the point in which $d_l = d_r$ in the function seen below (Eq. 4). Additionally, the points lying along the adjacent banks (P_l , P_r) are connected through a series of line segments, which are put through iterative search techniques within the R Code to define a point that is equidistant from the adjacent banks, further outlining the centerline. These search techniques within R are used to connect a point on one bank with 3 points on the adjacent bank. The first being a point lying directly across from the point of interest, the second being the point farthest upstream, and third being the farthest downstream point (Davies & Woodroffe, 2010). Additionally, the widths are calculated within the R Code by using an approximated tangent to the newly created centerline, which has the same direction as a vector defined as $P_c^+ - P_c^-$. P_c is the point of interest (where the width is being defined) and the plus and minus variation of this variable are the points directly upstream and downstream of the point of interest, respectively. Perpendicular to this approximate tangent is a line that is approximately normal to the centerline at P_c. This line segment is used to define a straight line (l_n) which passes through P_c and can be defined as the width of the channel at P_c (Davies & Woodroffe, 2010). These calculations are based on Equation 1 discussed previously. The convergence length is defined in this project as the distance in which the estuary (from the mouth, moving landward) moves from a funnel shape to a river. The R Code uses the relationship between the distance from the mouth and the width

at each set of corresponding points along the banks to create an exponential fit curve, where the width of an estuary is delineated per unit of distance upstream of the mouth of the estuary, giving an approximate length in which the convergence reaches its maximum distance.

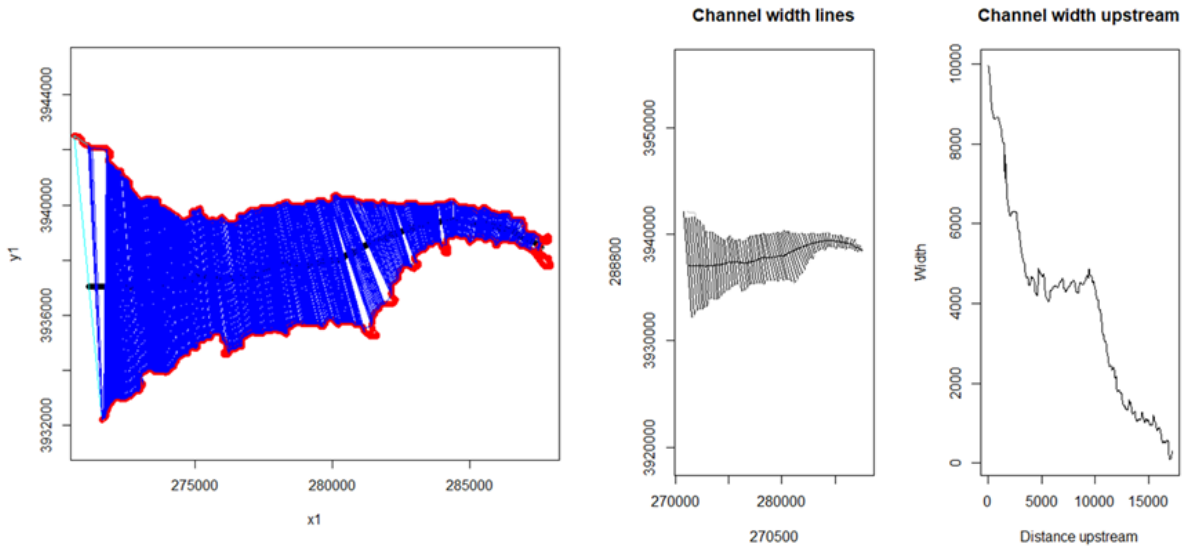

Figure 4 Graphic depiction of the data processing executed in R (E28). The graph on the left depicts the lines drawn within the estuary, estimating width at each distance variable. The line graph on the far right depicts the channel width per distance variable.

(4) $$f(\alpha) = \alpha P_l + (1-\alpha)P_r,\ \alpha \in [0,1]$$

Where, *F(0)* is the centerline, which was found using the uniroot function in R.

3.4. Statistical Significance Tests

To test the statistical significance, two tests were performed in R. The first of these was a t-test, comparing the width measurements from 1985 and 2015 from each estuary. This was done by first saving each width array as a .csv file by using the command: 'write.csv(width, "'estuary'_'year'_width.csv")', where 'estuary' is the estuary identification number and 'year'

specifies which year the widths correspond. Then, using an unpaired t-test, the widths were compared between the two years using the following command: 't.test(width_0_85,width_0_15,paired=FALSE)', where the two widths arrays are the x and y variables and 'paired' indicates whether the samples are paired or not. In this case, since the sample sizes are not equal, 'paired' is given the argument of FALSE. This was done for each estuary pair. The second test performed was the KS test to determine if the distribution of widths is the same for each estuary pair. The data used for this was the previously created .csv files containing the width data. However, these first needed to be converted into vector datasets. This was done within the command for the KS test: 'ks.test(as.vector(t(width_0_85)), as.vector(t(width_0_15)), alternative = "two.sided")', where the width arrays are the x and y variables and 'alternative' indicates the alternative hypothesis. The alternative hypothesis in this case is that the distribution is two-sided, i.e. that the distributions of the widths in x and y are not equal. Estuary pairs were considered significantly different (1985-2015) if both the t-test and KS test showed significant differences in mean widths and width distributions, respectively.

3.5. Visual Analysis of Diminished Estuaries

During the result analysis portion of this project, it was determined that 4 estuaries were identified using the Hodder (2018) updated process in the year 1985, but were no longer being identified as estuaries using the same process in the year 2015. A visual analysis of these areas was conducted using the satellite imagery and the historical imagery function within Google Earth. From this analysis, it was decided that the estuaries would still be included as having been impacted by anthropogenic land use change as it can be seen in the imagery as it changes from 1985 to 2015. However, as there are no 2015 data for these areas, they cannot be quantified, or deemed statistically valid for the purposes of this research.

4. RESULTS

For the year 1985, there were 90 polygons provided by the updated Hodder (2018) process and 91 for the year 2015, representing possible estuaries identified by that model and then run through the ModelBuilder tool. Upon visual inspection of the polygons, 36 of the polygons were estuaries, and 44 were coastal embayments. The selection process consisted of determining whether the polygon was encompassing an estuary or an embayment by comparing the satellite imagery of the area with the boundaries of the polygon. If the polygon only captured the outer 'bay' area of the estuaries and not the associated estuarine tributary, it was considered an embayment (Fig. 5). Of these 36 polygons, 15 were processed successfully through the R Code (Fig. 6); 4 of these 15 polygons were identified as estuaries in 1985, but were not identified as estuaries in 2015, following the definition identified as a parameter of this study. Analyses of the other 21 estuary polygons using the algorithm resulted in errors, which will be discussed at length in the limitations section below.

Figure 5 Example of embayment which was excluded from the study.

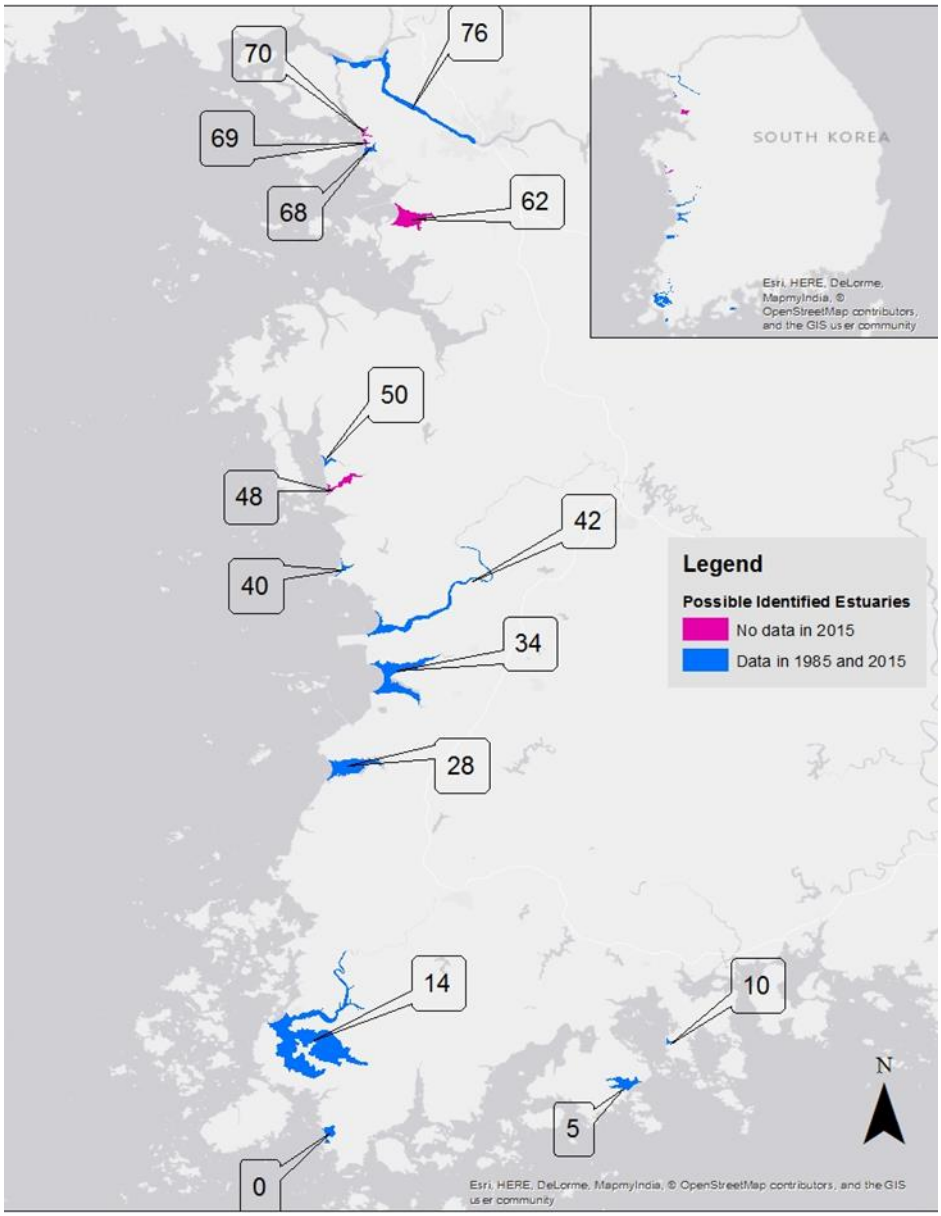

Figure 6 Map identifying the locations of the estuaries that were successfully processed in the R Code. The pink color indicates estuaries which only had data in 1985, while the blue color indicates estuaries with data in 1985 and 2015.

Model outputs for the convergence length and area change calculations for the 15 estuaries where full calculations were possible are presented in Table 1. Table 1 shows the 11 estuaries where area and convergence length changes could be computed for both 1985 and 2015

and for which comparisons could be made. Of these estuaries, 8 decreased in convergence length, ranging from -2% to -27% change in convergence length and -64% to 15% change in area, averaging a net decrease of 13% in convergence length and -17% in area. However, these results include changes that were not found to be statistically significant, so using only the 4 estuaries with statistically significant results for decreasing convergence lengths, the change ranges from -4% to -27% in convergence length and a -2% to -64% change in area averaging a net change of -16% in convergence length and -35% in area. The estuaries where convergence length increases ranged from 2% - 23% and a -50% to 9% change in area, with an overall net decrease in area of 24% and an increase in convergence length of 11%. These 3 estuaries all had statistically significant results. Estuaries E48, E62, E69, and E70 were identified in 1985, but due to changes in their shorelines, the algorithm could not delineate these estuaries in 2015. Figure 7 highlights these changes.

Estuary Set	1985 Number	2015 Number	85 Convergence (m)	15 Convergence (m)	Convergence Change	85 Area (sq. m)	15 Area (sq. m)	Area Change
E0	0	0	2107	2040	-3%	4093	3746	-8%
E5*	5	4	3104	2751	-11%	4838	4761	-2%
E10	10	10	957	838	-12%	2165	2272	5%
E14*	14	18	26440	19172	-27%	9161	7299	-20%
E28	28	32	6921	6750	-2%	7123	8205	15%
E34*	34	38	6721	6890	2%	11333	5693	-50%
E40*	40	43	1487	1141	-23%	5802	2064	-64%
E42*	42	46	21892	23873	9%	8759	9517	9%
E48	48	No Longer Exists	22637	--	--	2789	--	--
E50*	50	54	1453	1391	-4%	4108	1930	-53%
E62	62	No Longer Exists	4295	--	--	7278	--	--
E68*	68	69	1708	2100	23%	3308	2303	-30%
E69	69	No Longer Exists	761	--	--	1770	--	--
E70	70	No Longer Exists	1168	--	--	1422	--	--
E76	76	75	151399	117212	-22%	3392	3212	-5%

Table 1 List of the change in convergence and area for each estuary set. * signifies sets that were significant for both the KS test and the t-test.

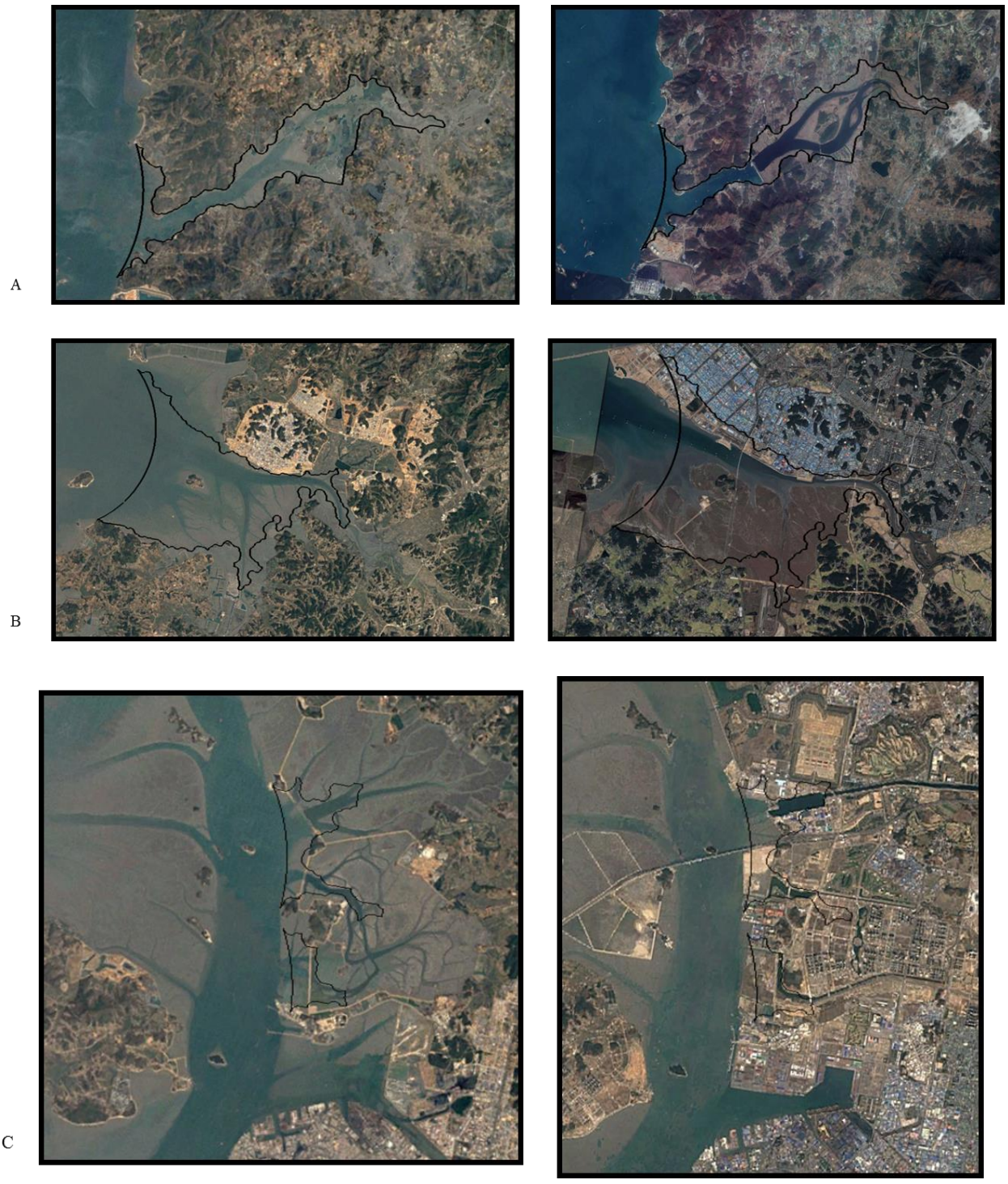

Figure 7 Google Earth satellite imagery of the changes in estuaries without 2015 identification. For each set of images, 1985 is on the left and 2015 is on the right. The black outline indicates the position of the estuary as it was in 1985. It is placed in both time periods for reference. A) E48; B) E62; C) E69 to the south and E70 to the north (included in the same image as they are part of the same estuarine system).

4.1. Statistical Validity

The statistical validity of each set of estuaries was tested. The 4 estuaries that were not identified in 2015 as estuaries were excluded from this portion of the project, as there is no 2015 width data to compare with the 1985 width data. As they were excluded from the statistical analysis, a visual analysis was performed on these estuaries using Google Earth satellite imagery (Fig. 7). Out of the 11 estuaries with data in both time points, 7 of the estuary sets were significant at the $p < 0.005$ significance level for the t-test. For these sets (E5, E14, E34, E40, E42, E50, E68), the significance indicates that we can reject the null hypothesis, meaning that there is a statistically significant difference in the means of the width data; it is therefore assumed that the change in convergence length and area can be considered significant. The other 4 sets (E0, E10, E28, E76), were not significant ($p > 0.05$) when tested using the t-test, indicating that we fail to reject the null hypothesis and that the widths were not significantly different from 1985 to 2015. In general, this result indicates that not much change occurred between the two time points.

When tested using the KS test, 8 of the 11 estuary sets were found to be significant at the $p < 0.005$ level. For these sets (E5, E14, E28, E34, E40, E42, E50, E68), the significance indicates that the null hypothesis that the distributions are equal can be rejected. This result strengthens the statistical validity that changes occurred within the estuary. For this reason, only the estuaries that were found to be significant in both tests have been analyzed for the changes in convergence length and area. These sets include: E5, E14, E34, E40, E42, E50, and E68 (Fig. 8). An interesting conclusion from the statistical tests is that the tests ruled out polygons that are not true estuaries, or estuaries with very little change between the two time

points. These estuaries were either found not significant for either one or both tests conducted. This increases confidence in the overall process.

	T-test Values		KS test Values
Estuary Set	*t*	*p*-value	*p*-value
E0	0.487	0.627	0.193
E5*	-3.857	**0.000**	**0.000**
E14*	14.743	**0.000**	**0.000**
E10	0.187	0.852	0.514
E28	-0.996	0.319	**0.000**
E34*	17.533	**0.000**	**0.000**
E40*	9.464	**0.000**	**0.000**
E42*	-3.360	**0.001**	**0.000**
E50*	4.340	**0.000**	**0.000**
E68*	4.235	**0.000**	**0.000**
E76	-0.298	0.766	**0.001**

Table 2 This table reports the results of the t-tests and KS test for each estuary set. The significant p-values are indicated, as well as the estuaries which were significant in both tests. The t-value is an indicator of the size of the difference in means relative to the variation in the means, the larger the t-value, the less likely the null hypothesis is correct, meaning there is a more significant difference in the means. A negative t-value indicates that the mean of the second group (2015, in this case) is less than the mean of the first group (1985).

Figure 8 Location of estuaries that were analyzed, due to their statistically significant changes.

4.2. Dam Location

For the 7 estuaries being analyzed and the 4 estuaries which could not be included- due to there not being a 2015 polygon to analyze- there were dams located within the tidal portion of

each estuary, except E68 (Fig. 9). Estuary E68, which did not have a dam added, was heavily impacted by land reclamation along the estuary banks.

Figure 9 Location of dams relative to the analyzed estuaries. E68 is impacted more heavily by land reclamation as there are no dams present in the area.

5. DISCUSSION

The results of the analyzed estuaries support the hypothesis that changes have occurred within the estuaries on the Korean Peninsula. The estuary sets will be discussed individually as the changes are unique for each case. The sets to be discussed are E5, E14, E34, E40, E42, E50, and E68 as these are the estuaries which passed both statistical validity tests. In addition, the estuaries which no 2015 data were obtained are included in the discussion.

One important thing to note before the discussion of each estuary is that due to some issues with data resolution that will be discussed in the limitations section, a few of the analyzed estuaries were analyzed according to the former estuarine area (i.e. the area identified in 1985). This was done because when a dam is installed in an estuary, the area above the dam is transformed into a freshwater lake. However, the algorithm used for 2015 identification of the estuary does not separate out areas above the dam (i.e. the freshwater lakes) as part of the estuary. Consequently, in this thesis, these former portions of the estuary will still be considered in this analysis. During this portion of the discussion, the term freshwater lake will refer to the area upstream of the dam. The measured convergence lengths are used to measure shoreline change in the former estuarine beds, particularly in the estuaries which were no longer identified in 2015.

5.1. E5 Estuary Set

The Google Earth satellite imagery for this estuary set (Fig. 10) indicates there was a dam built across the E5 estuary prior to 1985, so the changes to be discussed have occurred post-dam construction, from 1985 to 2015. This damming converted roughly 11% of the estuary into a freshwater lake. However, analysis results show that within the 30-year period, statistically

significant changes have occurred within this estuary. By 2015 the analyses found a small decrease in area (about 2%) and an 11.4% decrease in convergence length. This is roughly equivalent to a loss of 2.5 km^2 of estuary, in terms of shoreline change within the former estuarine system. These changes are likely primarily the result of increased sedimentation associated with the installation of the dam and land reclamation projects.

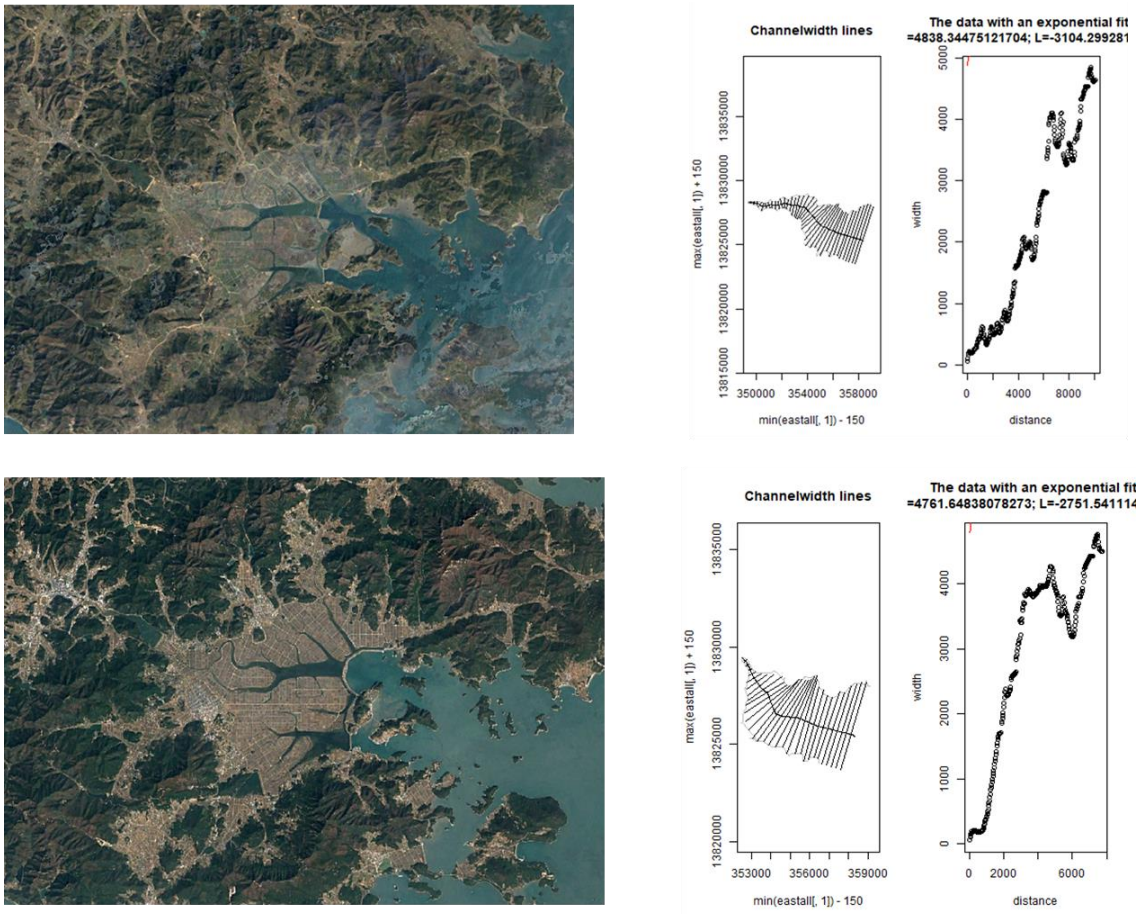

Figure 10 E5 estuary Google Earth satellite imagery from 1985 (top) to 2015 (bottom). The associated R Plots for each year are to the right of the satellite images.

5.2. E14 Estuary Set (South Yeongsan Estuary)

In 1985, the South Yeongsan Estuary was characterized by extensive mudflats along its banks, which extended into the estuary about 2 kilometers on either side. By 1986, anthropogenic structures were built along the edges of the estuary, near the mouth. These were in preparation for the dam that was added across the mouth in 1991, which converted 76% of the estuarine area to freshwater lake. Land reclamation projects began along the areas that were once mudflats. The analysis of this estuary indicates that by the year 2015, the damming of the estuary and the subsequent land reclamation projects claimed 20% of the original estuarine area. This change is roughly equivalent to a loss of 82 km^2 of estuary within the former estuarine system. Additionally, there was a 27% decrease found in the convergence length. These changes are primarily the result of land reclamation, coupled with the increased sedimentation rate caused by a reduction of water flow after the installation of the dam and the land reclamation.

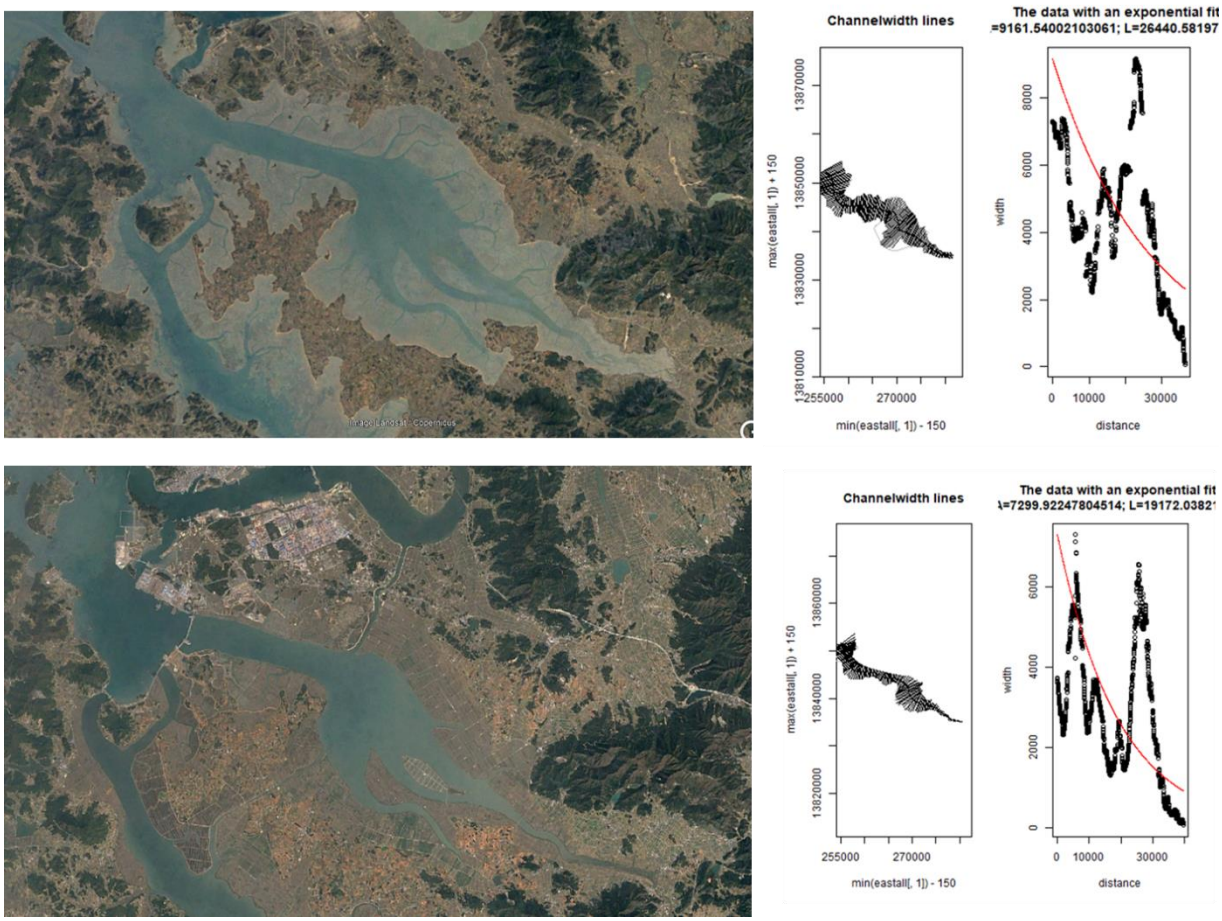

Figure 11 South Yeongsan estuary in 1985 (top) and 2015 (bottom). The associated R Plots for each year are to the right of the satellite images.

5.3. E34 Estuary Set (Saemangeum Estuary)

The results indicate that the convergence length of this estuary increased, while the area decreased. The 33km long Saemangeum Dam was constructed across the mouth of the Saemangeum Estuary, starting in 1994 and was completed in 2006, making it the largest sea dike in the world. The installation of the Saemangeum Dam was coupled with extensive land reclamation within the lake/estuary of the tidal flats. Although originally closed off to form a freshwater lake, the dam was opened to allow a restricted influx of seawater, allowing this

system to return to estuarine conditions. The construction of this offshore dam led to the gradual build of sediment within the lake/estuary over time. Because the dam restricts the natural flow of the estuary, the system was not as efficient in flushing out the sediment, expanding the already existing tidal flats. Because of these structures, the estuary began shrinking, further impeding the natural flow of sediment through the system. In the 30-year time span between 1985 and 2015, the Saemangeum Estuary lost 50% of its area, equivalent to 29 km^2 of former estuarine area. This large reduction in such a short period of time caused a rapid reduction in the tidal prism of the estuary, causing the estuary to continue retaining sediment. This created a negative feedback loop, which caused the natural estuary to change entirely. Figure 12 below depicts the change between the two time periods studied, 1985 and 2015.

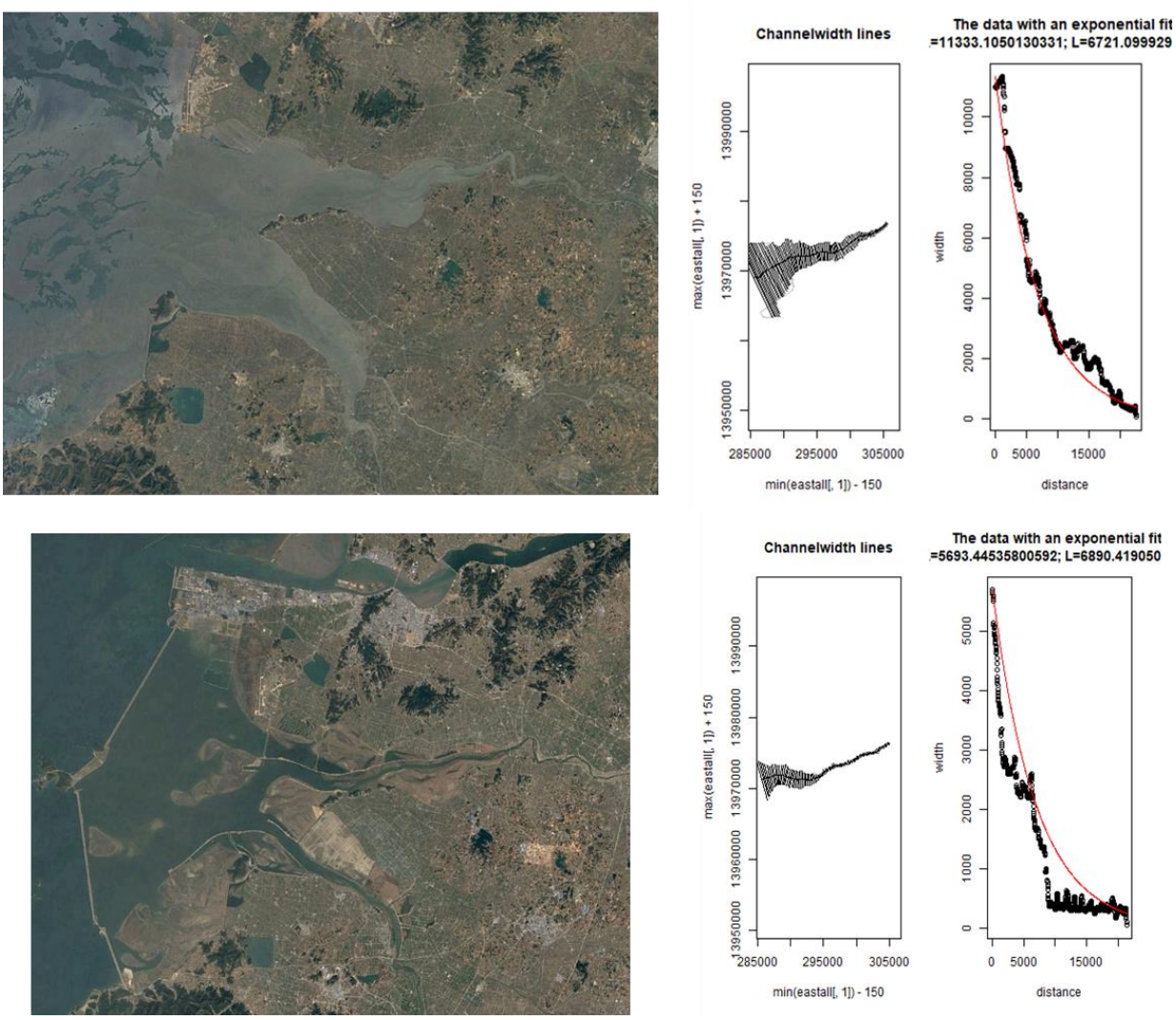

Figure 12 Saemangeum estuary from 1985 (top) to 2015 (bottom). The associated R Plots for each year are to the right of the satellite images.

5.4. E40 Estuary Set (Daechon Estuary)

This estuary set is very similar to the Saemangeum Estuary (E34). In 1985, this estuary contained a series of mud flats (Fig. 13). In 1987, the construction of an offshore dam began, which was completed in 1988, converting the entire estuary into a freshwater lake. By 1989, sediment started building up at the mouth of the former estuary, as the system was unable to

flush the sediment out naturally. Land reclamation projects started as early as 1990, including the construction of seawalls along the boundaries of the reclaimed land. The decrease in both the convergence length and the area of the former estuarine system, in just 3 decades indicates that the estuary is shrinking over time, due to the increased sedimentation rate. Overall, this estuary lost 64% of its total area (about 3.5 km^2) with evident changes to the natural hydrologic function and flow regime.

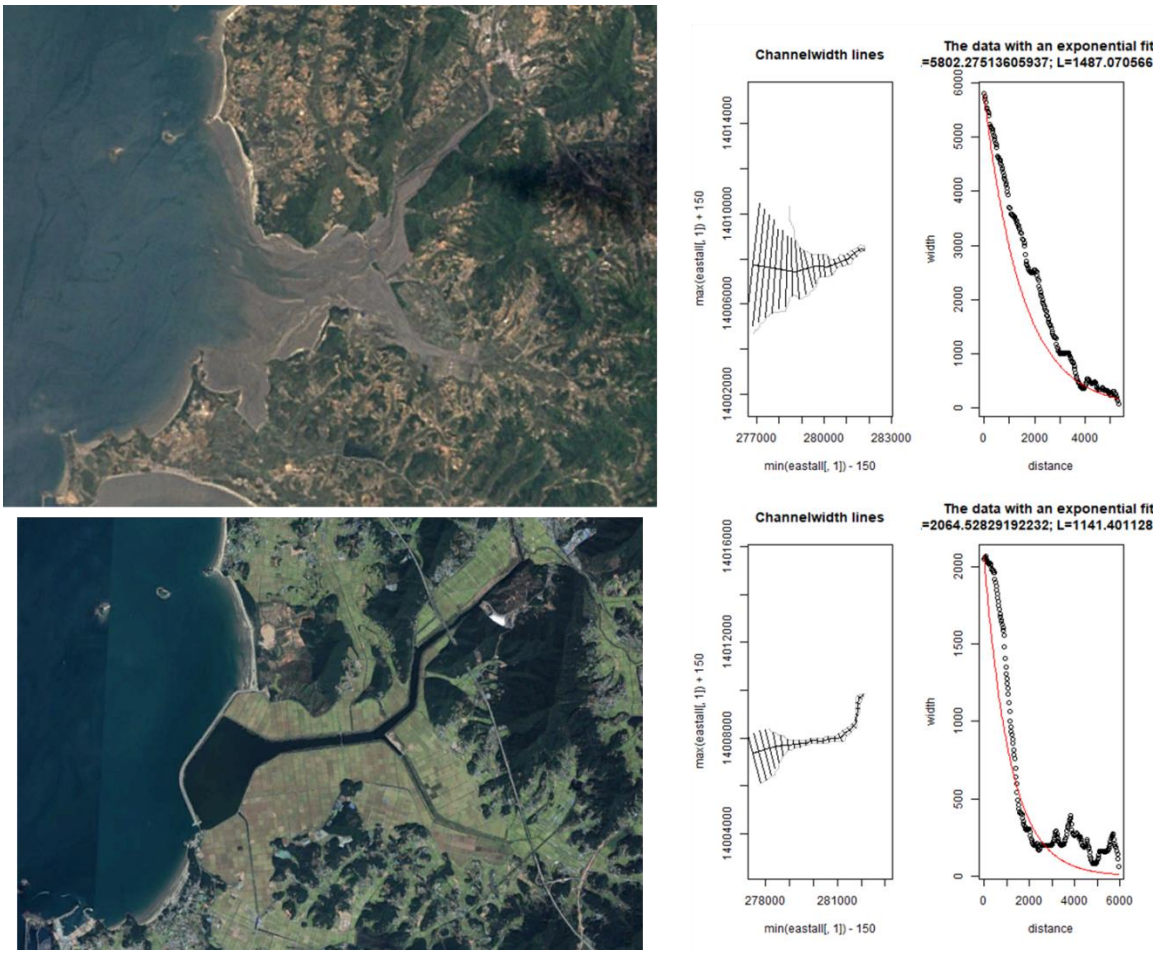

Figure 13 Daecheon estuary from 1985 (top) to 2015 (bottom). The associated R Plots for each year are to the right of the satellite images.

5.5. E42 Estuary Set (Geum Estuary)

This estuary presents an interesting case. In 1985, a little over 8 kilometers upstream of the mouth, construction on an estuarine dam had just started (Fig. 14) and was completed in 1988. This damming action converted 54% of the former estuary to freshwater lake, above the dam. Immediately after it was finished, sediment began building up directly behind the dam and in areas farther upstream. In addition to this, a tributary just downstream of the newly constructed dam continued flushing sediment into the estuary, which eventually settled and built up as the flow of water was restricted by the dam. By 2015, water flow was severely cut off by the 1988 dam, causing water to pool behind the dam, leading to flooding in areas directly behind this structure. The convergence length and area analyses encompass the area of the 1985 estuary, consequently, and for the 2015 analyses, spans the dam. The convergence length of this estuary increased, which is indicative of a shrinking estuary. The former estuary lost 1.2 km^2 of surface area. However, the area also increased due to the creation of an additional 8 km^2 of freshwater lake, above the dam, and shoaling below the dam due to the loss of the tidal prism. The increase in area is primarily due to the pooling of water directly behind the dam, while the increased convergence length is indicative of the increased sedimentation rate experienced below the dam, causing the estuary to shrink.

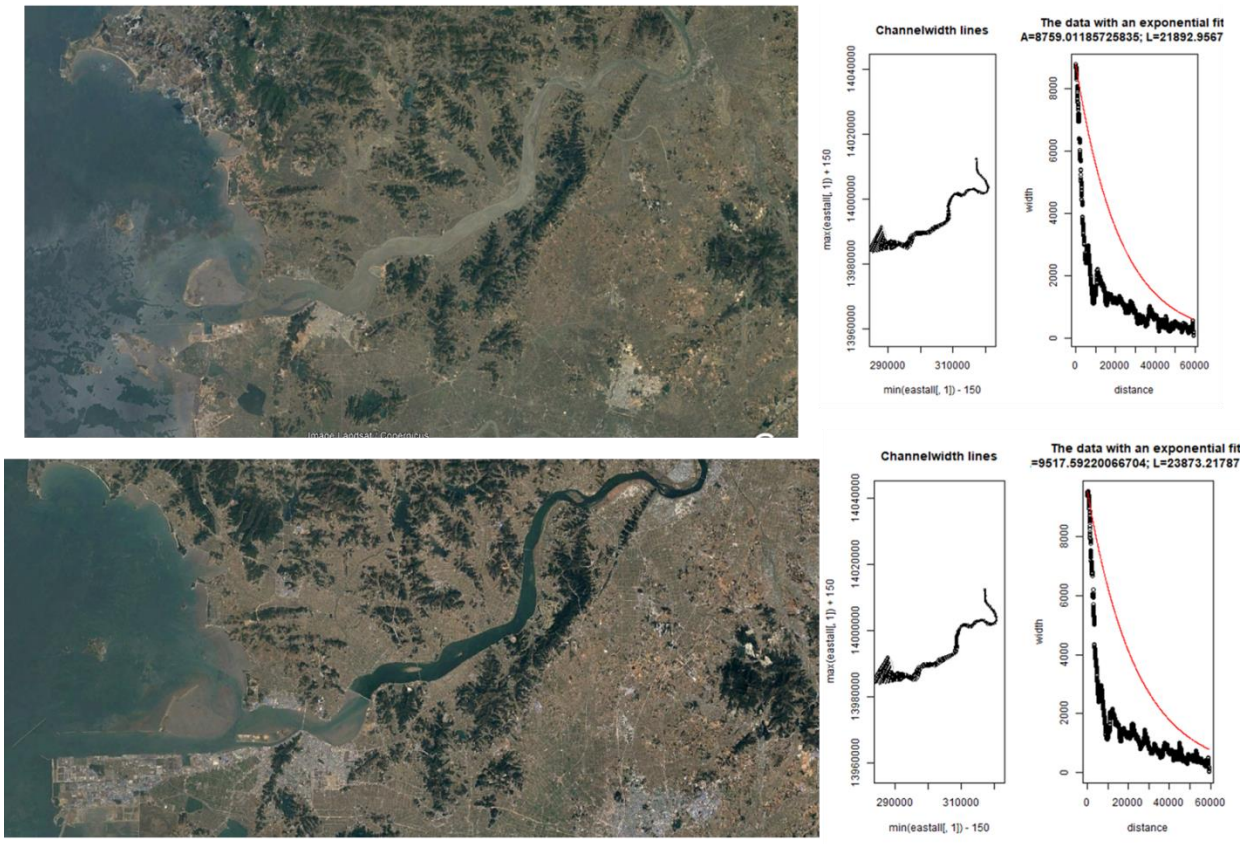

Figure 14 Geum estuary from 1985 (top) to 2015 (bottom). The associated R Plots are to the right of the satellite images.

5.6. E48 1985 Estuary

In 1985, this estuary contained extensive mudflats (Fig. 15). In 1994, land reclamation projects were started in preparation for dam construction, which was completed in 1998. This dam was located about 3 kilometers upstream of the mouth of the estuary. In 1999, a second dam was built upstream of the first dam. The convergence analysis for 2015 was not possible because the dam created the loss of roughly 72% of the 1985 estuary.

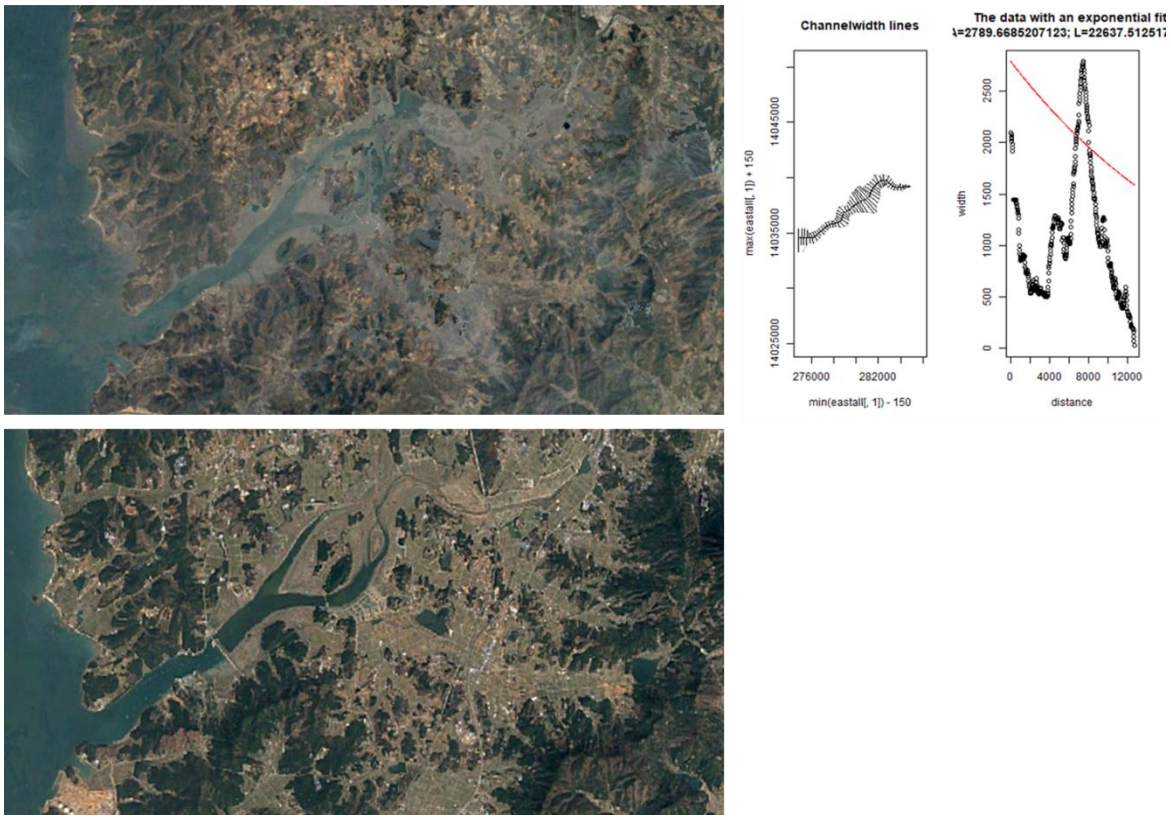

Figure 15 The E48 estuary in 1985 (top) and 2015 (bottom). The associated R Plot for 1985 is to the right of the satellite image.

5.7. E50 Estuary Set

From 1994 to 2000, an estuarine dam was constructed along the mouth of the estuary, converting the entire estuary into a freshwater lake. By the end of the year 2000, increased sedimentation rates filled in a majority of the upstream portion of the former estuarine area. In addition to this, localized shoaling features appeared closer to the mouth of the estuary, further decreasing the size of the estuary. By 2015, increased sedimentation due to the restricted flushing of the system caused by the estuarine dam reduced the area of the former estuary by 53%, decreasing the convergence length. This is equivalent to a loss of 1.7 km^2 of former estuary. Figure 16 highlights the changes between the two analyzed years, 1985 and 2015.

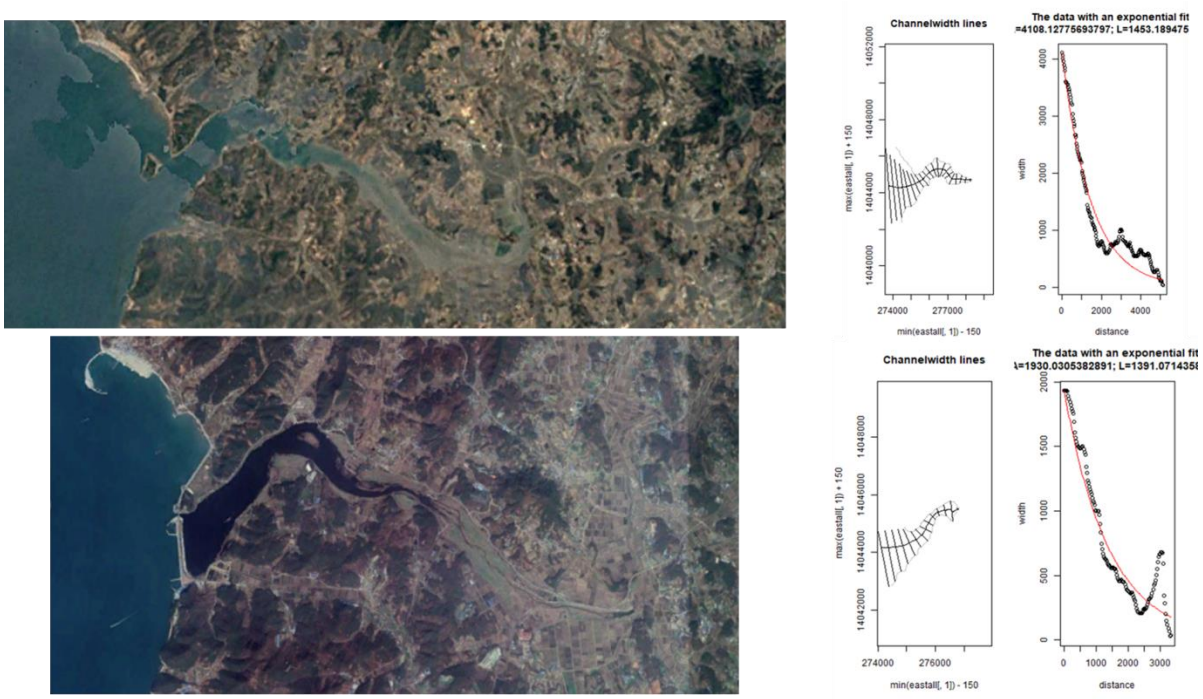

Figure 16 E50 estuary in 1985 (top) and 2015 (bottom). The associated R Plots for each year are to the right of the satellite images.

5.8. E62 Estuary Set (Hwacheon Estuary)

In 1985, this estuary was largely a natural system with no estuarine dams, however, with some existing land reclamation around the city of Ansan. In 1989 a large portion of the tidal flats along northern shoreline were reclaimed. From this reclamation project, an offshore dam was built across the mouth of the estuary, which was completed in 1994, converting the entire estuary into a freshwater lake. By 2015, major land reclamation took place along the boundaries of the estuary, which included the building of seawalls along the edges of the reclaimed land. This led to enhanced sedimentation, cutting off the river flow connection to the estuary/lake. This caused the estuary/lake to not be identified in 2015, leading to the inability to quantify the changes that have occurred as a result of the addition of these anthropogenic structures. Figure

17 highlights the changes within the estuary from 1985 to 2015.

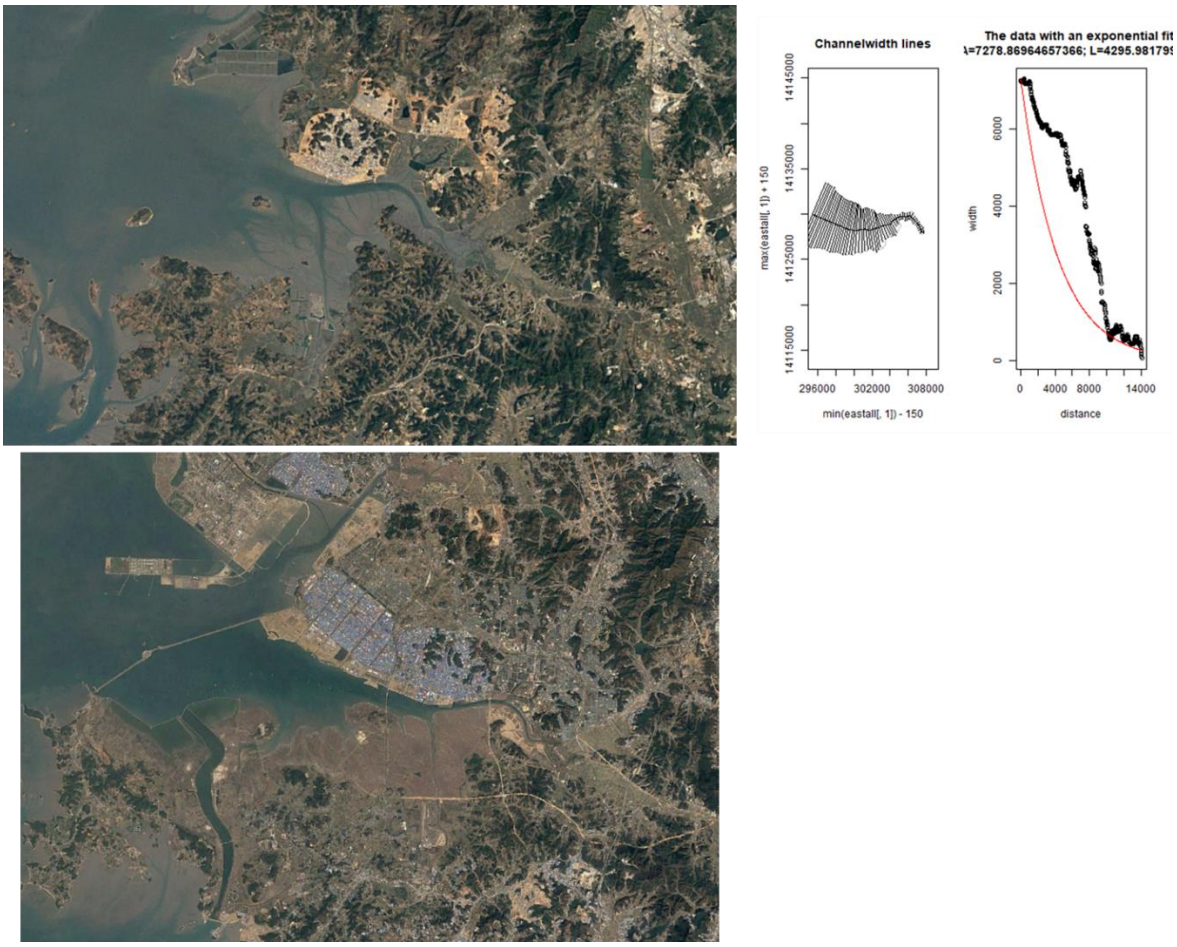

Figure 17 Hwacheon estuary from 1985 (top) to 2015 (bottom). The associated R Plot for the year 1985 is to the right of the satellite image.

5.9. E68 Estuary Set

The series of estuaries comprises the North Harbor area of the extensive Port of Incheon, consequently, the area had already undergone extensive alterations prior to 1985 and comprises some of the most extensive anthropogenic alterations of any of the estuarine systems in this

study (Fig. 18). This area contained an estimated 35 km^2 of mudflats in 1985, according to Google Earth satellite imagery. That same year, several built structures began influencing and changing the geomorphology of the estuary. These structures include dams and seawalls around portions of the estuary to increase sediment build up for land reclamation projects. By 1988, these projects claimed 30% of the area of this estuarine system (equivalent to about 2.8 km^2 of former estuary), permanently altering sedimentation and water flow regimes. This, in turn, increased the convergence length. The extent of modification to this estuary is so extensive that it is hard to distinguish where the water flow is even occurring. In fact, this area is where 2 of the 4 estuaries that were unaccounted for in 2015 are located. This area is so heavily modified that an estimated 24 km^2 of mud flat within the original estuarine area were transformed into reclaimed land by 1989.

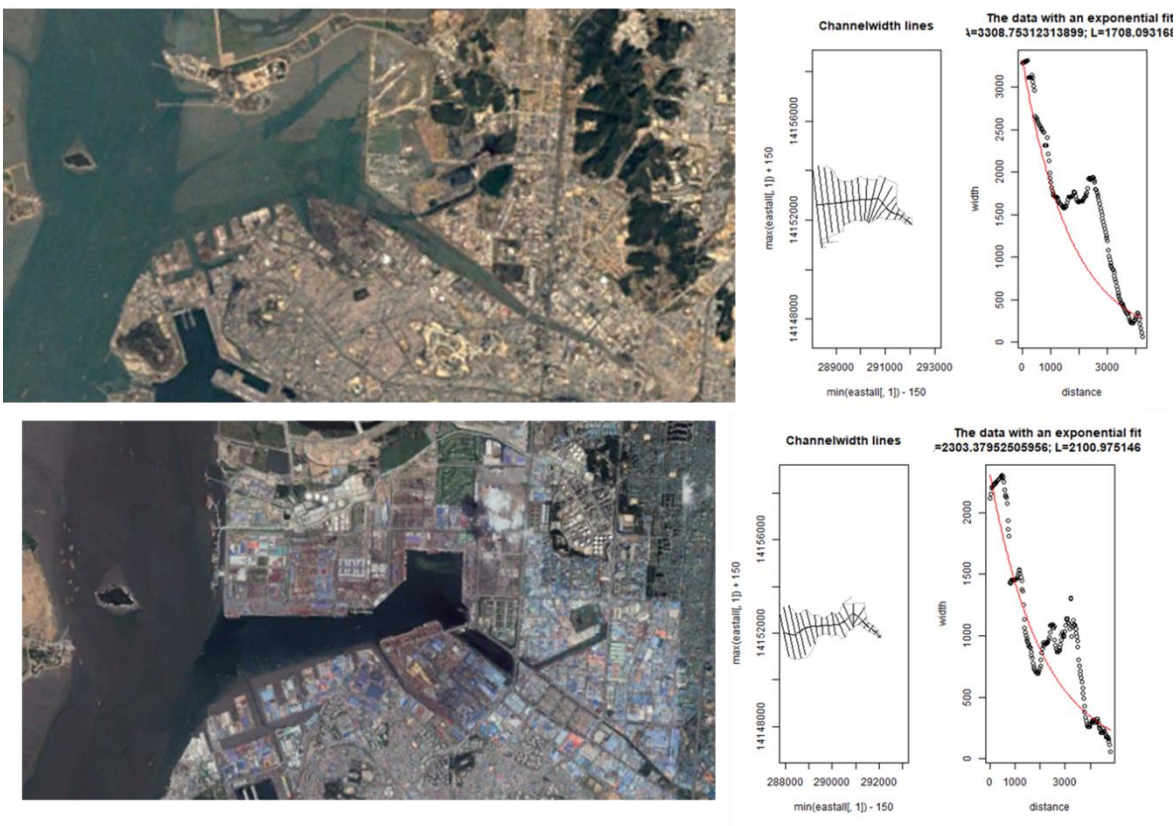

Figure 18 E68 estuary from 1985 (top) to 2015 (bottom). The associated R Plots for each year are found to the right of the satellite images.

5.10. E69 and E70 1985 Estuaries

These two estuaries are located in the same estuarine system as the E68 set of estuaries, within the greater Port of Incheon. The combined area of these estuaries is a little over 3 km^2. In 1984, no dams existed along the mouth of these estuaries, but by the end of 1985, at least 3 dams were built, trapping both estuaries in entirely (Fig. 19). In 1988, the entire estuarine area was completely filled in as part of an extensive land reclamation project. These estuaries were reduced from expansive mudflat systems to housing in a matter of three years. Although this cannot be quantified and put through the statistical validity tests, there are still visual changes

that can be observed through Google Earth satellite imagery. It is still apparent from these estuaries that the addition of anthropogenic structures eliminates the natural estuarine functions.

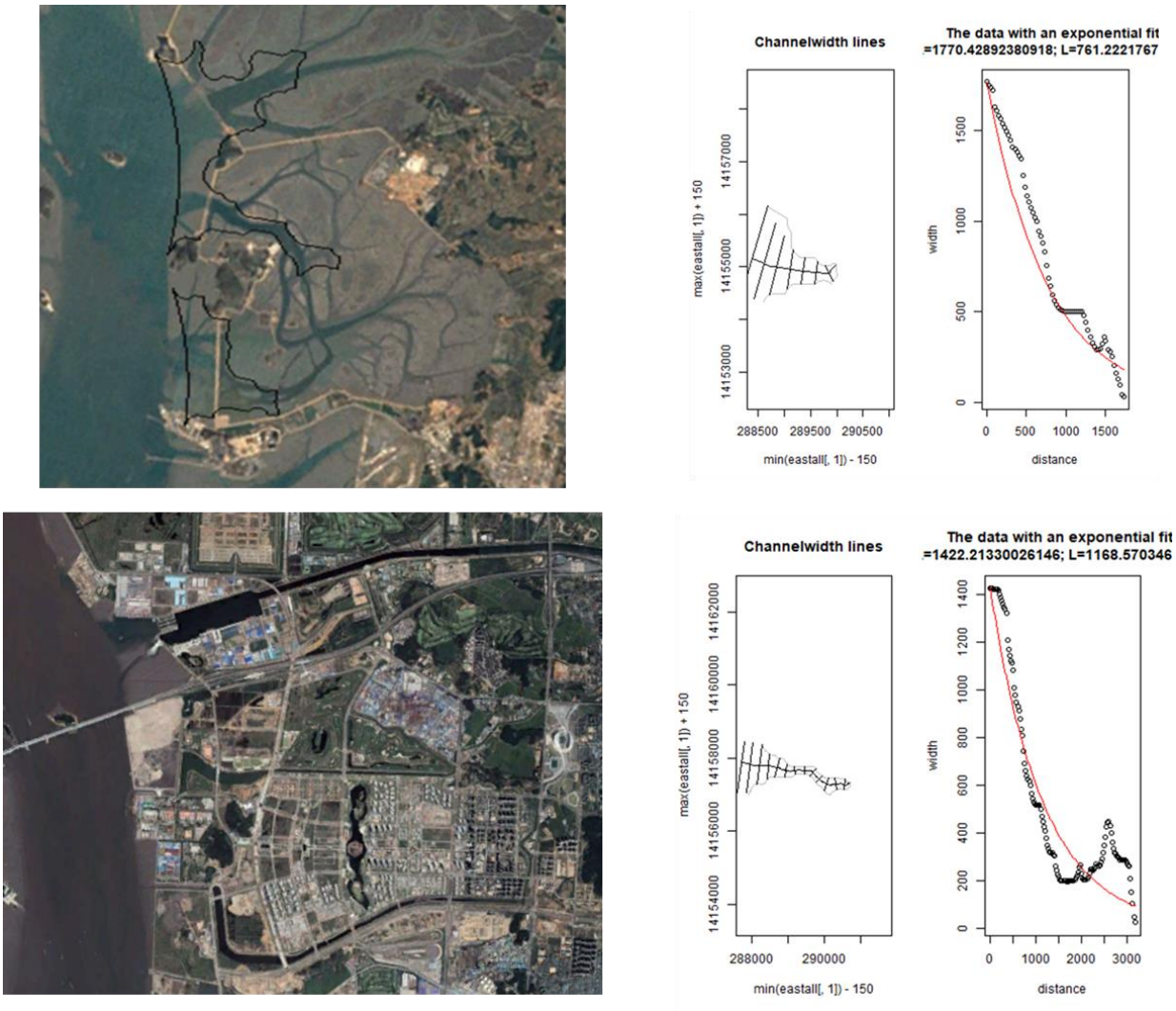

Figure 19 E69 estuary (to the south) and E70 estuary (to the north) are delineated in the top picture (from 1985). The picture on the bottom depicts their relative location in 2015. The R Plots for E69 (top) and E70 (bottom) for the year 1985 are to the right of the satellite images.

5.11. Assessment of Metric

Overall, the metric had success in measuring convergence length of estuarine systems. This metric is related to the traditional model discussed previously (Eq. 1), in the sense that the same nonlinear factors were made negligible in both measurements (i.e. depth, discharge, etc.). The present metric is comparatively similar to the traditional model in that it relies solely on the geometric widths of the estuary. Instead of viewing the changing geomorphology from a physical process standpoint, which relies on data collected by ground-truthing (this data may change depending on various factors), the metric used in this study views the geomorphology strictly from a geometric lens (which can easily account for changes on a frequent basis). By relying solely on widths collected via satellite imagery and geography, this eliminates the need to even include factors such as depth. This width-dependent measurement is valuable as a metric of calculating convergence length because convergence length is simply a quantification of the narrowing of the estuarine channels and by using only the widths to perform this task, the metric eliminates the need for complicated mathematical computations.

5.12. Implications

There are many implications resulting from the damming of an estuary, which are found throughout the entire estuarine ecosystem. Immediately after damming, the loss of freshwater input into the areas downstream of the dam affects the biological resources directly. The loss of biological resources directly impacts the local economy. Additionally, the loss of associated estuarine habitats and associated wetlands can have detrimental impacts on the coastal ecosystem and system functioning, including commercial fisheries and ultimately impact the economy.

Freshwater input is important in maintaining salinity levels within an estuary, as well as supporting effective fisheries management practices. After dam installation, the flow regime is

shifted and, depending on where the dam is installed, the salinity ranges from the areas downstream of the dam will shift as well, potentially impacting the benthic and epifaunal communities. Additionally, large sections of estuarine and salt marsh above the dam are completely lost, reducing the total amount of habitat and nursery grounds. The disruption of the benthic-pelagic coupling within the system leads to a loss of biodiversity.

As Williams et al. (2013 and 2014) demonstrated, the installation of the dam results in the reduction of the tidal prism below the dam, which results in a dramatic increase in sedimentation rates, which can increase by a factor of ten or greater, resulting in sedimentation rates of up to several centimeters per year. Within estuaries, it has been demonstrated (Norkko et al., 2002; Cummings et al., 2003; Hewitt et al., 2003; and Thrush et al., 2003a&b; Thrush et al., 2004), that a critical threshold of episodic deposition of 2 cm or more will rapidly create anaerobic conditions within the seabed, resulting in the death of the resident faunal community. The benthic and pelagic coupling within an estuary is central to the nutrient cycling and overall productivity of the system and an interruption of this coupling resulting from elevated sedimentation rates can have dramatic impacts on the entire ecosystem (Eyre and Ferguson, 2006) and potentially result in ecosystem collapse.

However, there are also significant benefits to the installation of the estuarine dams. They can provide hydroelectric power, provide the impoundment of freshwater for municipal, industrial and agricultural usage, control river flooding and prevent upstream storm surge and tsunami propagation. In addition, the reclaimed land due to land reclamation can also provide significant economic benefits as these lands are sold and developed.

5.13. Implications of this Research to Texas

The implications of the installation of estuarine dams can easily be applied to any system with comparable proposed alterations. One example would be the proposed Ike Dike project. The proposed project includes adding on to the existing Galveston seawall and creating flood gates for the Galveston Bay tidal inlet between Galveston Island and Bolivar Peninsula. The project will require the partial closing off of the tidal inlet, with a proposed reduction of the tidal prism by 30%. However, if the tidal prism is reduced by 30%, there will be a correlated reduction in the efficiency of the tidal flushing, which would likely result in a dramatic increase in sedimentation within the bay until a new equilibrium is established. This enhanced sedimentation could potentially result in the partial burying of existing oyster beds and alterations of the salinity gradient within the bay. Approximately 18% of the US wild catch oysters come from Galveston Bay (Haby et al., 2009), and it was demonstrated that during the flooding due to Hurricane Harvey, that the alteration of the salinity gradient in the bay resulted in nearly 100% die off of oysters on many of the most significant oyster beds in the bay (Du et al., 2019, Du et al., in prep.). A 30% loss of tidal prism will potentially have a detrimental impact to the oyster reefs within the bay, both impacting a vital economic resource as well as a vitally important component of the ecosystem. Additionally, the loss of tidal prism will significantly elevate the sedimentation rates within the bay, resulting in an increase to dredging costs and channel and harbor maintenance.

Although the Ike Dike will protect against major storm surge events, it cannot protect against major flooding due to rain events; in fact, it would exacerbate the flooding issues experienced in the Greater Houston Area. If the flood gates are closed for storm surge, but the

Houston area is experiencing intense rainfall, the additional water added to the system will be trapped within the bay, enhancing flooding within the bay and watershed.

5.14. Limitations

The biggest limitation experienced throughout the course of this research is the instability of the R Code. Several estuaries had errors while being processed through the code block. Some of these errors were manually avoided by deleting rows of null data in the width and distance arrays. However, a second error that occurred was not so easily avoided. Because the code was customized by Davies and not by the primary researcher on this project, it was complicated to follow and identify the sections of code causing this second error. It is believed by the primary researcher on this project that the second error is caused by estuaries with odd shapes, which are primarily formed around a rocky, or hilly, coastline. This error excluded 12 estuaries identified by the updated Hodder process (Hodder, 2018). In addition to this, 5 estuaries with multiple branches, or 'arms', could not be included in the analysis as the R Code arbitrarily chose different branches to run for each time point. For example, if an estuary had 2 branches and the first branch was processed by the R Code for the 1985 polygon, but the second branch was processed for the 2015 R Code, this estuary was excluded.

Additionally, there were data limitations for this project. Specifically, during the estuary identification process, the vectorization of surface water used (developed with the Hodder (2018) method and utilizing Global Surface Water Dataset and the HydroSHEDS data) is currently limited to a 100-meter resolution. When the algorithm selects embayments based on their proximity to rivers and streams, it will trace the boundaries of that embayment up to the point at which the resolution, or cell size, of the data is less than 100 meters. Theoretically, if a dam is built, the upstream portion of the body of water being identified should no longer be considered

as part of that estuary and the polygon boundaries around the embayment should stop at the dam location (i.e. should not include the freshwater lake portions of the former estuarine bed). However, using the 100-m resolution data limits this because a dam with a width smaller than 100-m may be skipped over if there is stream data on the other side that is larger than the 100-m resolution. Additionally, one of the preprocessing steps used to clean the surface water data prior to analysis via the modified Hodder (2018) workflow may cause embayment polygons to "jump" even slightly wider barriers, up to approximately 200 m. To overcome these limitations, for future work, the researcher is in the process of using 30-m resolution data in place of the 100-m resolution data; however, the portion of the modified Hodder (2018) workflow built using ArcGIS model builder software must be updated to process this type of data at 30-m resolution.

6. CONCLUSION

This study demonstrates that the process created to identify and quantify changes within estuaries on the Korean Peninsula can be accomplished, but would be greatly benefited by additional modifications. Overall, the 7 estuaries analyzed in the process and the 4 estuaries visually analyzed along with these, indicate that anthropogenic changes to land use and hydrologic flow can cause statistically measurable morphological changes. In some cases, such as the 4 visually analyzed estuaries, these anthropogenic changes resulted in the complete loss of the estuarine system as a whole. As a result of the total loss of each of these estuaries due to anthropogenic alterations, the algorithm correctly ceased to recognize these as estuarine systems in the 2015 data-base.

The analyses conducted in this study focused on morphological changes to these estuarine systems. However, the implications of the results of this study extend beyond simple morphological changes because these changes have associated loss of habitat and disruption of the ecosystem services provided by these estuaries. These services include: storm buffering services, biological services (i.e. hatching ground, ecosystem provision for breeding and feeding, etc.), and social and economic services. In addition to these, the benthic communities are impacted by the increased sedimentation experienced upon addition of dams. The reduction of these fragile systems raises the question of how this impacts the entire coastal ocean ecosystem associated with the estuary. Further research into this will need to be conducted in order to understand not just the geomorphological impact of shrinking estuaries, but the environmental impacts as well.

The next step for this project is to identify and correct the errors of the R Code. Once this is done, the process will be rerun to include all estuaries within the Korean Peninsula. After this is completed, the hope is to take this process to a global scale, to quantify the changes within estuaries globally. A global inventory of estuaries is what is needed to fully understand how anthropogenic structures are impacting these systems, and in turn, how this impacts society as a whole.

REFERENCES

Barbier, E. B., Hacker, S. D., Kennedy, C., Koch, E. W., Stier, A. C., & Silliman, B. R. (2011). The value of estuarine and coastal ecosystem services. *Ecological monographs*, *81*(2), 169-193.

Chang, H. (2008). Spatial analysis of water quality trends in the Han River basin, South Korea. *Water Research, 42*(13), 3285-3304.

Chappell, J., & Woodroffe, C. D. (1994). Macrotidal estuaries. *Coastal evolution: Late Quaternary shoreline morphodynamics*, 187-218.

Choi, I. C., Shin, H. J., Nguyen, T., & Tenhunen, J. (2017). Water policy reforms in South Korea: A historical review and ongoing challenges for sustainable water governance and management. *Water*, *9*(9), 717.

Chou, L. M., Yu, J. Y., & Loh, T. L. (2004). Impacts of sedimentation on soft-bottom benthic communities in the southern islands of Singapore. *Hydrobiologia*, *515*(1-3), 91-106.

Crawford, G.W., Lee, G.-A., 2003. Agricultural origins in the Korean Peninsula. Antiquity 999 77, 87.

Davies, G., & Woodroffe, C. D. (2010). Tidal estuary width convergence: Theory and form in North Australian estuaries. *Earth Surface Processes and Landforms: The Journal of the British Geomorphological Research Group*, *35*(7), 737-749.

Dronkers, J. (2017). Convergence of estuarine channels. *Continental Shelf Research, 144*, 120 133**.**

Du, J., Park, K., Dellapenna, T. M., & Clay, J. M. (2019). Dramatic hydrodynamic and sedimentary responses in Galveston Bay and adjacent inner shelf to Hurricane Harvey. *Science of the Total Environment*, *653*, 554-564.

Du J, Park K, Dellapenna TM (in prep.) Extreme precipitation and slow salinity recovery after Hurricane Harvey led to massive oyster kill in Galveston Bay.

Evans, G., & Prego, R. (2003). Rias, estuaries and incised valleys: is a ria an estuary? *Marine Geology*, *196*(3-4), 171-175.

Eyre, B. D., & Ferguson, A. J. (2006). Impact of a flood event on benthic and pelagic coupling in a sub-tropical east Australian estuary (Brunswick). *Estuarine, Coastal and Shelf Science*, *66*(1-2), 111-122.

Fairbridge, R. W. (1968). RIA, RIAS COAST AND RELATED FORMS Ria, rias coast and related forms. In *Geomorphology*(pp. 942-944). Springer, Berlin, Heidelberg.

Gao, J. H., Jia, J., Kettner, A. J., Xing, F., Wang, Y. P., Li, J., Gao, S. (2015). Reservoir-induced changes to fluvial fluxes and their downstream impacts on sedimentary processes: The Changjiang (Yangtze) River, China. Quaternary International.

Haby MG, Miget RJ, Falconer LL (2009) Hurricane damage sustained by the oyster industry and the oyster reefs across the Galveston Bay system with recovery recommendations. TAMU-SG-09-201, A Texas AgriLife Extension Service / Sea Grant Extension Program Staff Paper, The Texas A&M University System, College Station, TX, 51 p.

Hewitt, J. E., Cummings, V. J., Ellis, J. I., Funnell, G., Norkko, A., Talley, T. S., & Thrush, S. F. (2003). The role of waves in the colonisation of terrestrial sediments deposited in the marine environment. *Journal of Experimental Marine Biology and Ecology*, *290*(1), 19-47.

Hume, T. M., Snelder, T., Weatherhead, M., & Liefting, R. (2007). A controlling factor approach to estuary classification. *Ocean & Coastal Management*, *50*(11-12), 905-929.

Jeong, S., Yeon, K., Hur, Y., & Oh, K. (2010). Salinity intrusion characteristics analysis using EFDC model in the downstream of Geum River. *Journal of Environmental Sciences*, *22*(6), 934-939.

Langbein, W. B. (1963). The hydraulic geometry of a shallow estuary. *Hydrological Sciences Journal*, *8*(3), 84-94.

Lanzoni, S., & Seminara, G. (1998). On tide propagation in convergent estuaries. *Journal of Geophysical Research: Oceans*, *103*(C13), 30793-30812.

Lee K.-H., Rho, B.-H., Cho H.-J., Lee. C.-H., (2011). Estuary classification based on the characteristics of geomorphological features, natural habitat distributions and land uses. *Journal of the Korean Society for Oceanography, 16*, pp. 53-69

Little, S., Spencer, K. L., Schuttelaars, H. M., Millward, G. E., & Elliott, M. (2017). Unbounded boundaries and shifting baselines: Estuaries and coastal seas in a rapidly changing world.

Martínez, M. L., Intralawan, A., Vázquez, G., Pérez-Maqueo, O., Sutton, P., & Landgrave, R. (2007). The coasts of our world: Ecological, economic and social importance. *Ecological Economics*, *63*(2-3), 254-272.

Nassar, M. A. (2011). Multi-parametric sensitivity analysis of CCHE2D for channel flow simulations in Nile River. *Journal of hydro-environment research*, *5*(3), 187-195.

Norkko, A., Thrush, S. F., Hewitt, J. E., Cummings, V. J., Norkko, J., Ellis, J. I., ... & MacDonald, I. (2002). Smothering of estuarine sandflats by terrigenous clay: the role of wind-wave disturbance and bioturbation in site-dependent macrofaunal recovery. *Marine Ecology Progress Series*, *234*, 23-42.

O'meara, T. A., Hillman, J. R., & Thrush, S. F. (2017). Rising tides, cumulative impacts and cascading changes to estuarine ecosystem functions. *Scientific Reports*, *7*(1), 10218.

Park, S. S., & Lee, Y. S. (2002). A water quality modeling study of the Nakdong River, Korea. *Ecological Modelling*, *152*(1), 65-75.

Pekel, J., Cottam, A., Gorelick, N., & Belward, A. S. (2016). High-resolution mapping of global surface water and its long-term changes. *Nature*, *540*(7633), 418-422.

Perillo, G. M. (1995). Chapter 2 Definitions and Geomorphologic Classifications of Estuaries. Developments in Sedimentology Geomorphology and Sedimentology of Estuaries, 17-47.

Pritchard, D. W. (1952). Salinity distribution and circulation in the Chesapeake Bay estuarine system. *Journal of Marine Research*, *11*(2), 106-123.

Savenije, H. H. (2006). *Salinity and tides in alluvial estuaries*. Elsevier.

Thrush, S. F., Hewitt, J. E., Norkko, A., Nicholls, P. E., Funnell, G. A., & Ellis, J. I. (2003a). Habitat change in estuaries: predicting broad-scale responses of intertidal macrofauna to sediment mud content. *Marine Ecology Progress Series*, *263*, 101-112.

Thrush, S. F., Hewitt, J. E., Norkko, A., Cummings, V. J., & Funnell, G. A. (2003b). Macrobenthic recovery processes following catastrophic sedimentation on estuarine sandflats. *Ecological Applications*, *13*(5), 1433-1455.

Thrush, S. F., Hewitt, J. E., Cummings, V. J., Ellis, J. I., Hatton, C., Lohrer, A., & Norkko, A. (2004). Muddy waters: elevating sediment input to coastal and estuarine habitats. *Frontiers in Ecology and the Environment*, *2*(6), 299-306.

Wells, J. T., Adams, C. E., Park, Y., & Frankenberg, E. W. (1990). Morphology, sedimentology and tidal channel processes on a high-tide-range mudflat, west coast of South Korea. *Marine Geology*, *95*(2), 111-130.

Williams J., Dellapenna, T.M., Lee, G-.H., Louchouarn, P., (2014). Sedimentary impacts of anthrpogenic alterations on the Yeongsan Estuary, South Korea. Marine Geology, 357, 256-271.

Williams, J. R., Dellapenna, T. M., & Lee, G. (2013). Shifts in depositional environments as a natural response to anthropogenic alterations: Nakdong Estuary, South Korea. Marine Geology, 343, 47-61.

Wolanski, E., Day, J. W., Elliott, M., & Ramesh, R. (Eds.). (2019). *Coasts and Estuaries: The Future*. Elsevier.

WWF. (2017). HydroSHEDS. Retrieved February 18, 2018, from http://hydrosheds.org/

Yoon, H.Y.H.S., Yoo, C.I., Na, W.B., Lee, I.C., Ryu, C.R.,(2007). Geomorphologic evolution and mobility of sand barriers in the Nakdong estuary, South Korea. Journal of 1124 Coastal Research 358–363.

Zhu, Q., Wang, Y. P., Gao, S., Zhang, J., Li, M., Yang, Y., & Gao, J. (2017). Modeling morphological change in anthropogenically controlled estuaries. *Anthropocene*, *17*, 70-83.